JOC The Journal of Organic Chemistry

Article

pubs.acs.org/joc

Switching of the Triplet Excited State of Styryl 2,6-Diiodo-Bodipy and Its Application in Acid-Activatable Singlet Oxygen Photosensitizing

Ling Huang, Wenbo Yang, and Jianzhang Zhao*

State Key Laboratory of Fine Chemicals, School of Chemical Engineering, Dalian University of Technology, Dalian 116024, China

Supporting Information

ABSTRACT: IodoBodipy-styrylBodipy dyads triplet photosensitizers were prepared (**B-1** and **B-2**) which contain acid-responsive moiety. Both compounds show broadband visible light absorption, due to the resonance energy transfer (RET) between the two different visible light-harvesting Bodipy units. The photophysical properties of the dyads were studied with steady-state and nanosecond time-resolved transient absorption spectroscopy. The production of triplet excited state is switched ON or OFF by protonation/deprotonation of the amino group in the dyads. In the neutral form, the excited state is short-lived (<10 ns) and no singlet oxygen ($^1O_2$) photosensitizing was observed. Upon protonation, a long-lived triplet excited state was observed (τ_T = 3.1 μs) and the $^1O_2$ quantum yield (Φ_Δ) is up to 73.8%. The energy levels of the components of the dyads were changed upon protonation and this energy level tuning exerts significant influence on the triplet state property of the dyad. Acid-activated shuffling of the localization of the triplet excited state between two components of a dyad was observed. Furthermore, we observed a rare example that a chromophore giving shorter absorption wavelength is acting as the singlet energy *acceptor* in RET. The experimental results were rationalized by density functional theory (DFT) and time-dependent DFT (TDDFT) calculations.

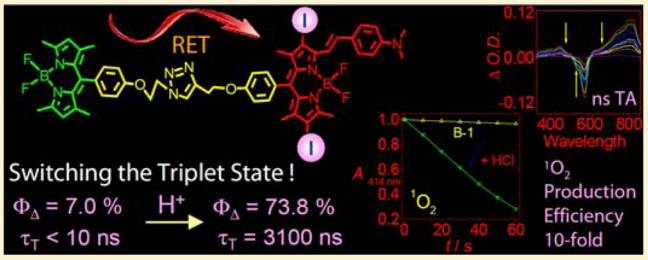

1. INTRODUCTION

Triplet photosensitizers have attracted much attention owing to the applications in photocatalysis,[1−6] photodynamic therapy and luminescent O_2 sensing,[7−14] and study of fundamental photochemistry.[6,15−18] Currently the investigations are focused on designing new chromophores that produce triplet excited state upon photoexcitation.[6,11] However, different from the switching of *singlet* excited states, such as by the renowned approaches of photoinduced electron transfer (PET),[19,20] the fluorescence resonance energy transfer (FRET),[21−25] or the through space/bond energy transfer (TBET),[26−32] the studies on switching of the *triplet* excited state of organic chromophores were rarely reported and the *switching* of the triplet excited state with external stimuli was not studied in detail with time-resolved transient spectroscopy.[7,9,33,34] Switching of the *singlet* excited states is extremely important for designing various functional molecular materials, such as fluorescent molecular probes, luminescent bioimaging reagents, light-harvesting molecular arrays, and molecular logic gates.[34] We envisage that the same holds true for switching of the *triplet* state, for example, the external stimuli-activated photosensitizers can be used as targeted photodynamic therapy (PDT) reagents to improve the selectivity and to reduce the side effect.[7,35]

Switching of the triplet state manifold of the Ru(II), Os(III), Re(I) coordination center with dithienylethene or stilbene moiety were reported,[36−39] but the switching of triplet state was not transduced to any photosensitizing applications. O'Shea et al. prepared aminophenyl bromo aza-Bodipy, for which the production of triplet excited state was inhibited by the photoinduced intramolecular electron transfer (PET).[7] Upon protonation, i.e., in acidic solution, the PET effect ceased and the intersystem crossing (ISC) of iodo-azaBodipy produces the triplet excited states upon photoexcitation; hence, pH-activated photodynamic therapy was achieved.[7] Other pH-activatable PDT reagents based on a similar mechanism have been reported; however, these triplet excited state switchings were not studied with time-resolved transient spectroscopy.[7,35] Recently Akkaya et al. demonstrated the singlet oxygen ($^1O_2$) photosensitizing ability of a Bodipy dyad is able to be switched by controlling the *direction* of FRET, which is modulated by protonation of the Bodipy chromophore.[33] It should be pointed out that the *inherent* triplet state property of the iodo-Bodipy was not modulated. Recently we prepared Bodipy dyads with one Bodipy unit iodinated.[40] Triplet excited state equilibrium was observed for the dyads, but no *switching* of the triplet excited state with external stimuli was achieved. Dyad or triad triplet photosensitizers with the RET effect was devised to achieve broadband absorption of visible light.[41,42] Some dyads/triads show the ping-pong singlet and triplet energy transfer,[42,43] but again the production of triplet excited state cannot be switched by external stimuli.[42] Moreover, switching of the triplet excited state production ability with the mechanism

Received: August 17, 2014
Published: October 3, 2014

Scheme 1. Synthesis of the Acid-Responsive Triplet Photosensitizers B-1−B-4 and the Compounds 1−6[a]

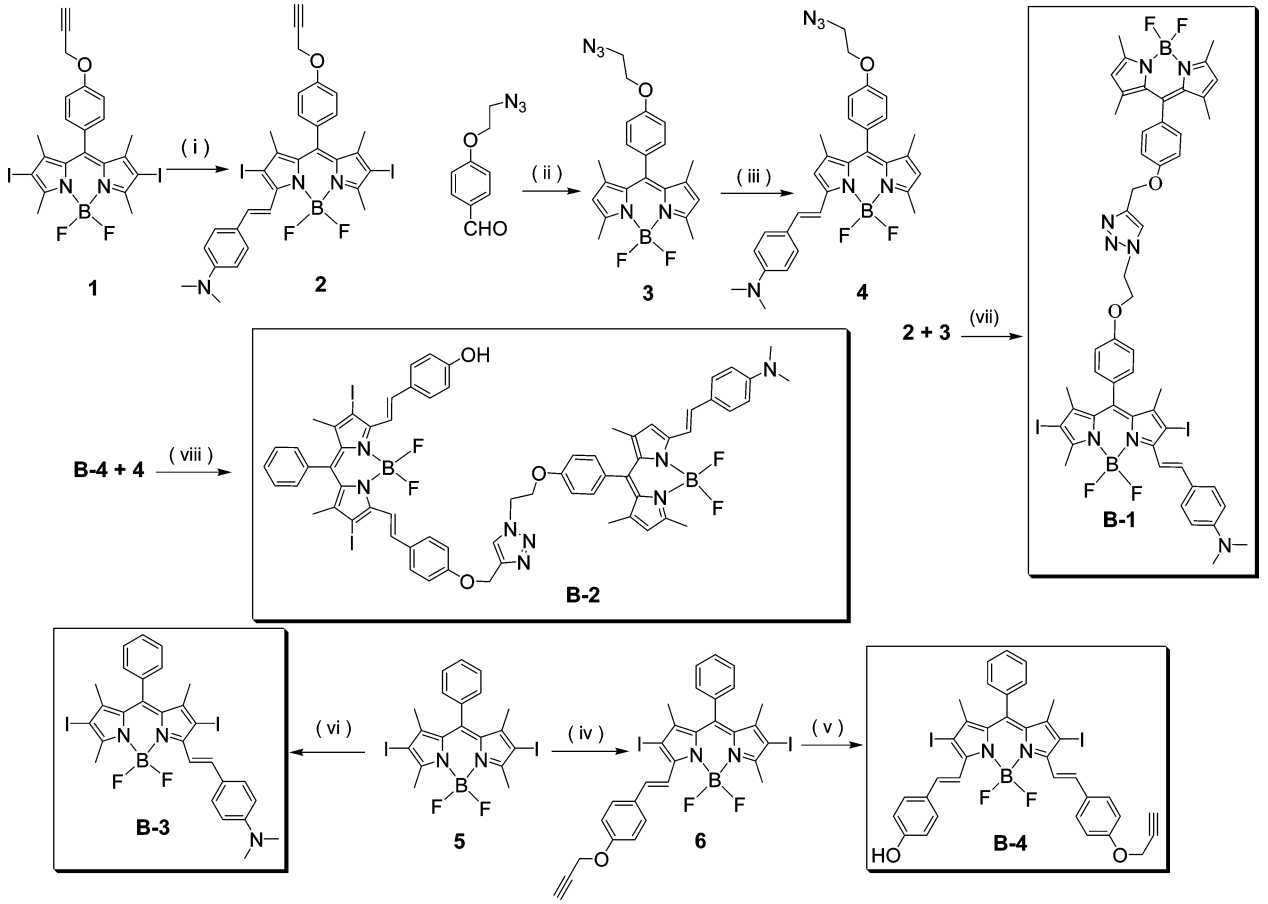

[a]Key: (i) 4-*N*,*N*-dimethylbenzaldehyde, toluene, acetic acid, piperidine, reflux, 4 h in Ar; yield: 57%. (ii) 2,4-Dimethylpyrrole, trifluoroacetic acid, DDQ, TEA, $BF_3{\cdot}Et_2O$, rt, 2 h, in Ar; yield: 21%. (iii) The same as step i, 12 h, in Ar; yield: 49%. (iv) 4-Propynylalkoxybenzaldehyde, toluene, acetic acid, piperidine, reflux, 0.5 h, in Ar; yield: 15%. (v) 4-Hydroxybenzaldehyde, toluene, acetic acid, piperidine, reflux, 0.5 h, in Ar; yield: 89%. (vi) The same as step i, reflux, 10 h, in Ar; yield: 62%. (vii) Et_3N, $CuSO_4{\cdot}5H_2O$, and sodium ascorbate, 24 h, at rt, in Ar; yield: 87%. (viii) The same as step vii, yield: 81%.

other than the above-mentioned was not reported. Hence much room is left to study the switching of the triplet excited states of organic photosensitizers.[6,11]

Herein we found that the *intrinsic* triplet excited state property of dimethylaminostyryl Bodipy can be switched by manipulation of the ICT effect of this chromophore. The switching of the triplet excited state of the dyads were investigated in detail with nanosecond time-resolved transient difference absorption spectroscopy as well as DFT/TDDFT calculations. In the neutral form of the chromophore, no triplet excited state was detected with nanosecond time-resolved transient absorption spectroscopy, and no $^1O_2$ was produced upon photoirradiation. With protonation, long-lived triplet excited state was observed and $^1O_2$ quantum yield (Φ_Δ) increased to 79.8%. Thus, we demonstrated that the modulation of the triplet excited state can be manifested in the ability to produce $^1O_2$. Moreover, we observed a rare example that the chromophore gives shorter absorption wavelength is acting as the singlet energy *acceptor* in the RET process, which is due to the larger Stokes shift of the chromophore. We also show that the ISC is unable to be inhibited by the competing FRET effect in a dyad, which is different from a previous study. With these studies, we extended the toolbox to switch the triplet excited state of organic chromophores as well as the studies on photochemistry of triplet photosensitizers.

2. RESULTS AND DISCUSSION

2.1. Design and Synthesis of the Compounds. Two Bodipy dyads **B-1** and **B-2** were designed (Scheme 1). Bodipy was selected as the chromophore due to its excellent photophysical properties, such as strong absorption of visible light, high fluorescence quantum yields, good photostability, and the feasibly derivatizable molecular structure.[22,44−54]

In **B-1**, the dimethylaminostyryl iodo-Bodipy is the singlet energy acceptor and the *spin converter*,[6,42,43,50−52,54] thus the triplet excited state can be produced by the ISC effect of this unit. On the other hand, the unsubstituted Bodipy part is the singlet energy donor. Since the two parts give different absorption maxima in the visible spectral region, broadband absorption of visible light is achieved. Besides excitation into the energy acceptor, excitation at shorter wavelength will also lead to triplet state production, via the singlet RET between these two components, and thereafter the ISC of the singlet energy acceptor (spin converter).[6,40−42,55,56] This molecular designing approach is different from the conventional triplet photosensitizers, in which only a single visible light-harvesting chromophore was used, thus there is only one major absorption

dx.doi.org/10.1021/jo5019014 | J. Org. Chem. 2014, 79, 10240−10255

band in visible spectral region.[7,35] In our case, the iodo-Bodipy part in **B-1** is the singlet energy acceptor, thus the effect of protonation on the *inherent* triplet state property of the chromophore can be studied. It should be pointed out that the triplet excited state of **B-1** is postulated to be localized on the styryl Bodipy part. The styryl Bodipy shows a lower T_1 state energy level than unsubstituted Bodipy.[42,43]

The designing of **B-2** (Scheme 1) is similar to that a molecular logic gate reported by Akkaya;[33] that is, the direction of the FRET can be switched by protonation of the aminostyryl Bodipy part. Different from **B-1**, the localization of the triplet excited state of **B-2** can possibly be switched by protonation. The T_1 state can localize on either the dimethylaminostyryl Bodipy part or the 4′-hydroxylphenyl Bodipy part. The switching process was studied with steady state and nanosecond time-resolved transient absorption spectroscopy. We found that the triplet excited state of **B-2** upon protonation is *delocalized* on both chromophores. In order to unambiguously assign the effect of the protonation on the triplet state property, compounds **B-3** and **B-4** were prepared as references for study of the photophysical properties as well as the application in $^1O_2$ photosensitizing.

2.2. UV–Visible Absorption and Fluorescence Emission Spectra. The UV–vis absorption spectra of **B-1** was studied (Figure 1). Two absorption bands at 499 and 635 nm

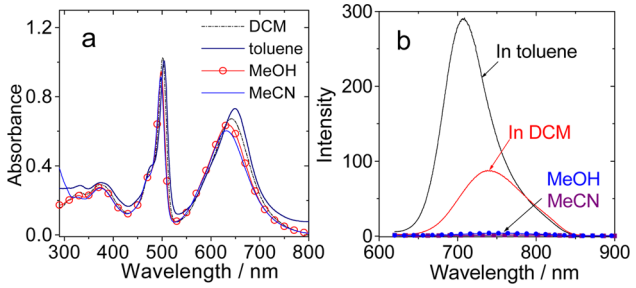

Figure 1. (a) UV–vis absorption spectra of **B-1** in dichloromethane (DCM), methanol, toluene, and acetonitrile. (b) Fluorescence emission spectra of the **B-1** in different solvents. λ_{ex} = 610 nm. c = 1.0×10^{-5} M, 20 °C.

were observed. The absorption band at 499 nm is attributed to the Bodipy part and the band at 635 nm is attributed to the 2,6-diiodo dimethylaminostyryl Bodipy part.[22,28,33,44,57] The absorption at 635 nm shows blue-shifting in polar solvents. Conversely, the absorption band at 499 nm is less sensitive to solvent polarity.[22,44]

The emission of **B-1** in different solvent were studied (Figure 1b). The emission of the Bodipy moiety at 520 nm disappeared in **B-1** (see the Supporting Information, Figure S25), which is due to the energy transfer to the iodo-styryl Bodipy, although electron transfer cannot be excluded.[27,33,58] Emission at 704 nm was observed, and the intensity is highly dependent on the solvent polarity (Figure 1b).[59] This emission band is substantially quenched in polar solvents compared with that in nonpolar solvents. For example, the emission at 704 nm in toluene is the strongest. In CH_2Cl_2 the emission intensity is reduced by half, and the emission was completely quenched in CH_3OH and CH_3CN. The polarity-dependent emission is attributed to the intramolecular charge transfer (ICT) effect, which is known to be more significant in polar solvents.[59]

The UV–vis absorption and fluorescence emission spectra of **B-2** in different solvents were studied (Figure 2a). The

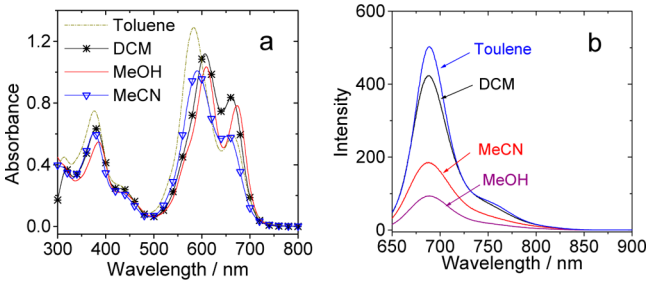

Figure 2. (a) UV–vis absorption spectra of **B-2** in DCM, methanol, toluene, and acetonitrile. (b) Fluorescence emission spectra of **B-2** in different solvents, λ_{ex} = 635 nm, c = 1.0×10^{-5} M, 20 °C.

absorption band at 595 nm was attributed to the dimethylamino styryl Bodipy part, supported by the UV–vis absorption of the reference compound **4** (see the Supporting Information, Figure S19). This result indicates that the iodo substituents induce red-shift in the absorption band (**B-1**).[60] The absorption band at 670 nm is attributed to the 4′-hydroxylphenyl Bodipy part.[33] The UV–vis absorption bands are dependent on the solvent polarity.

The fluorescence emission spectra of **B-2** in different solvents were studied (Figure 2b). The emission is centered at 689 nm, which is less sensitive to solvent polarity compared with **B-1**. Interestingly the emission intensity changed with variation of the solvent polarity, but the emission wavelength does not. Thus, the emission band is attributed to the 4′-hydroxylstyryl Bodipy part, confirmed by the emission feature of the reference compound **4** (see the Supporting Information, Figure S19). It is postulated that the variation of the emission intensity of **B-2** is due to the changing of the S_1 state energy level of the dimethylamino-styryl Bodipy moiety in **B-2**, which is dependent on the solvent polarity. The energy of the S_1 state of the emitter in **B-2** is not dependent on the solvent polarity. In polar solvents, the FRET is more efficient, thus the emission of 4-hydroxyl phenyl Bodipy part becomes weaker.[33] Here it is an interesting example that the dimethylamino styryl Bodipy part gives a shorter *absorption* wavelength but *longer* emission wavelength than the 4′-hydroxylphenyl Bodipy part, and this moiety acts as the singlet energy acceptor. This effect is due to the large Stokes shift of the dimethylamino styryl Bodipy moiety (Figure 3 and Supporting Information, Figure S19). Such observation is rare for FRET.[21]

In order to clearly reveal the energy level changes of the chromophores in **B-2**, the absorption/emission of the reference compounds **4** and **B-4** were studied in different solvent (Figure 3). It is clear that the emission wavelength of compound **4** was red-shifted significantly with the solvent switched from toluene (λ_{em} = 645 nm), dichloromethane (λ_{em} = 669 nm), methanol (λ_{em} = 682 nm) to acetonitrile (λ_{em} = 700 nm). However, no such red-shift of emission wavelength was observed for compound **B-4** (λ_{em} = 698, 695, 689, and 685 nm in the corresponding solvents, respectively). Notably the emission wavelength of compound **4** become longer than that of compound **B-4** with solvent polarity increased, i.e., the S_1 state energy level of compound **4** becomes lower than that of **B-4**. With these spectral data of the components of dyad **B-2**, we postulate that the emission of the **B-4** unit in **B-2** will be reduced due to the enhanced FRET to the singlet energy acceptor (with compound **4** as the analogue), yet the emission wavelength did not change because the emission is due to the iodo-styrylBodipy part in **B-2**, which is insensitive to solvent

dx.doi.org/10.1021/jo5019014 | J. Org. Chem. 2014, 79, 10240–10255

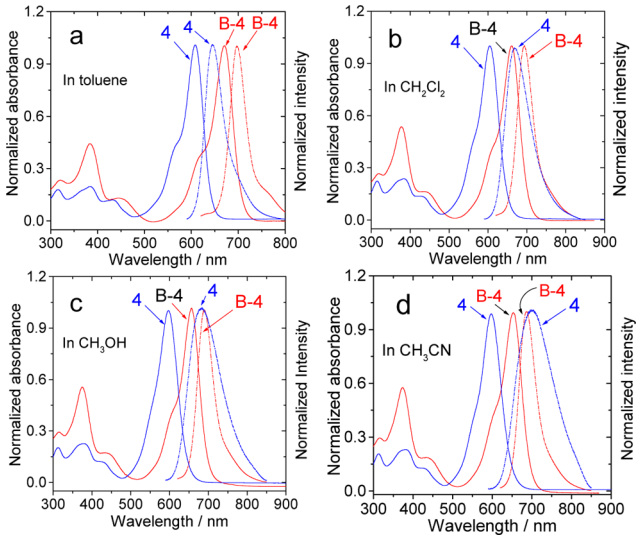

Figure 3. Normalized UV−vis absorption spectra (solid lines) and emission spectra (dashed lines) of **4** and **B-4** in different solvents of (a) toluene, (b) dichloromethane, (c) CH_3OH, and (d) MeCN. Different excitation wavelengths were used for **B-4** (λ_{ex} = 610 nm) and **4** (λ_{ex} = 580 nm). c = 1.0 × 10^{-5} M, 20 °C.

polarity (Figure 4d). These postulations were supported by the fluorescence excitation spectra (see later section).

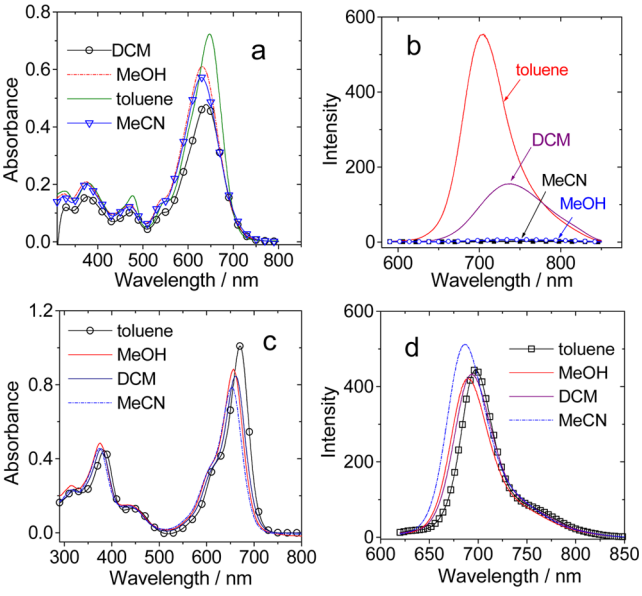

Figure 4. UV−vis absorption spectra of (a) **B-3** and (c) **B-4** in different solvents. Fluorescence emission spectra of (b) **B-3** (λ_{ex} =580 nm) and (d) **B-4** (λ_{ex} = 610 nm) in different solvents. c = 1.0 × 10^{-5} M, 20 °C.

The above analysis on the spectra of **B-1** was supported by the absorption and emission property of the reference **B-3** (Figure 4), for which the absorption band is slightly dependent on the solvent polarity and the emission intensity is highly dependent on the solvent polarity. This property is similar to the uniodinated dimethylamino styryl Bodipy compound.[59a] To rationalize the analysis of the spectral property of **B-2**, the emission of reference compound **B-4** is almost independent of the solvent polarity (Figure 4d). The photophysical properties of the compounds are listed in Table 1. **B-1**−**B-4** give weak fluorescence emission due to the ISC effect.

Table 1. Photophysical Parameters of B-1−B-4 and 4.[a]

	λ_{abs} (nm)	ε/ 10^5 M^{-1} cm^{-1}	λ_{em} (nm)	Φ_L[b] (%)	τ_T[c] (μs)	τ_F[d] (ns)
B-1	497/639	0.94/0.64	509	0.67	—[e]	—[e]
B-2	589/660	1.09/0.56	693	0.46	—[e]	1.28
B-3	631	0.65	—[e]	0.89	—[e]	—[e]
B-4	653	0.84	689	4.9	1.5	2.12
4	598	0.80	703	3.1	—[e]	0.87

[a]Recorded in CH_3CN/H_2O (9/1 v/v) at 20 °C. [b]Fluorescence quantum yield. [c]Triplet excited state lifetimes. Measured by nanosecond transient absorption in deaerated solutions. [d]Luminescent lifetimes, λ_{ex} = 472.6 nm (picosecond pulsed laser). [e]Not observed.

2.3. Variation of the UV−Visible Absorption and the Fluorescence Emissions Spectra Upon Protonation. In order to study the effect of protonation on the photophysical properties, the UV−vis absorption and the fluorescence emission spectra of **B-1** and the reference compound **B-3** were studied (Figure 5). Upon addition of aqueous HCl, thus

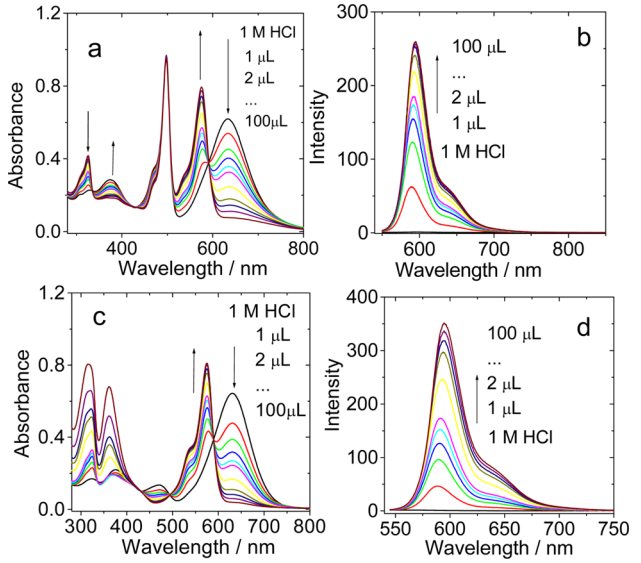

Figure 5. Variation of the UV−vis absorption spectra and the fluorescence emission spectra upon addition of aqueous HCl. (a) **B-1** with increasing HCl added and (b) the corresponding emission spectra changes of **B-1** (λ_{ex} = 540 nm). (c) **B-3** with increasing 1 M HCl added (d) the corresponding emission spectra changes of **B-3** (λ_{ex} = 540 nm). The aliquots of the HCl solution (1 M) added are 1, 2, 3, 4, 5, 10, 20, 30, 50, and 100 μL. In $MeCN/H_2O$ = 9:1(v/v). c = 1.0 × 10^{-5} M, 20 °C.

protonation of the amino group, the absorption band at 635 nm diminished and a new absorption band at 575 nm developed concomitantly (Figure 5a). The absorption band at 499 nm is hardly changed. In the UV region, the absorption band at 328 nm reduced and a new absorption band at 371 nm appeared. Isosbestic points at 592 and 428 nm were observed. These results indicated that the absorption band of the dimethylaminostyryl Bodipy shows blue-shifts upon protonation. This result is reasonable since the ICT effect will be diminished upon protonation of the amine substituents.[33,59]

dx.doi.org/10.1021/jo5019014 | J. Org. Chem. 2014, 79, 10240−10255

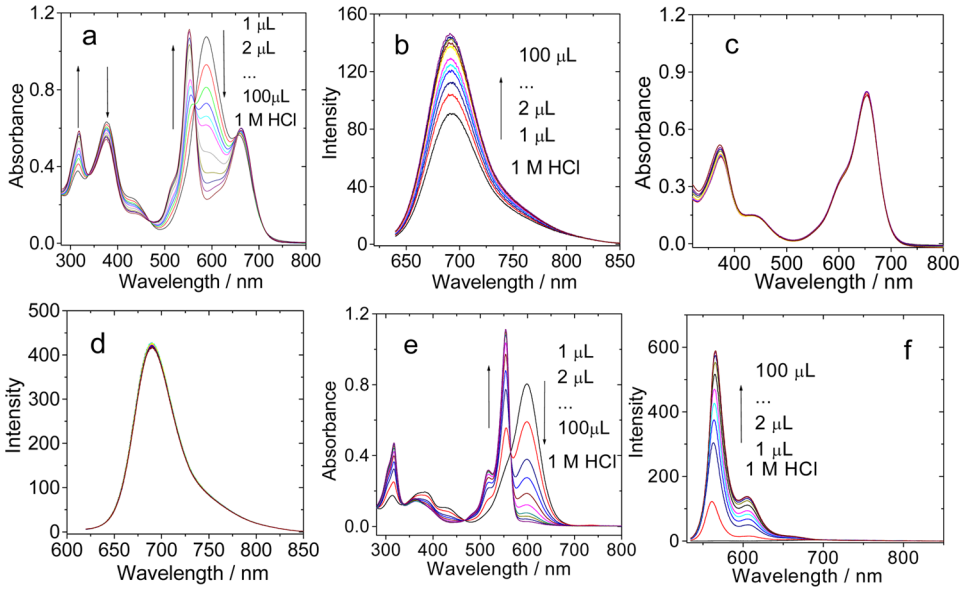

Figure 6. Variation of the UV−vis absorption and fluorescence emission spectra upon protonation with addition of aqueous HCl. (a) **B-2** upon titration with 1 M HCl and (b) the corresponding emission spectra changes (λ_{ex} = 630 nm); (c) **B-4** upon titration with 1 M HCl and (d) the corresponding emission spectra (λ_{ex} = 615 nm); (e) compound **4** upon titration with 1 M HCl and (f) the corresponding emission spectra changes (λ_{ex} = 530 nm). The aliquots of the HCl added are 1, 2, 3, 4, 5, 10, 20, 30, 50, and 100 μL. In MeCN/H_2O = 9:1 (v/v). $c = 1.0 \times 10^{-5}$ M, 20 °C.

The UV−vis absorption spectra and the fluorescence emission of **B-2** upon protonation were studied (Figure 6a,b). Upon protonation, the absorption band at 586 nm decreased and the absorption band at 552 nm intensified. The absorption band at 663 nm hardly gives any changes. The emission at 691 nm was intensified upon protonation. Different from **B-2**, the absorption spectra and the fluorescence emission spectra of **B-4** did not give any changes upon protonation (Figure 6c,d).

For **4**, the change of the UV−vis absorption spectra upon protonation is similar to that of **B-2** (Figure 6e). The emission band is at 560 nm, much shorter than that of **B-2** (Figure 6b). The emission of **4** was intensified upon protonation (Figure 6f). On the basis of these results, the increase of the emission intensity of **B-2** at 689 nm upon addition of acid is attributed to the elevated S_1 state energy level of the dimethylamino styryl Bodipy part upon protonation, thus diminishing the FRET from 4′-hydroxylstyryl Bodipy to the dimethylamino styryl Bodipy part, which imparts the quenching effect on the emission of **B-2**. As a result, the emission of 4′-hydroxylstyryl Bodipy part was intensified upon addition of aqueous HCl, in this case the FRET occurs, with singlet energy transfer from the dimethylamino styryl Bodipy part to the iodo-4′-hydroxylstyryl Bodipy part in **B-2**. The spectral changes upon protonation is reversible, the absorption and the emission is fully recovered after addition of base such as KOH (see the Supporting Information, Figures S52−S56).

2.4. Comparison of the Fluorescence Excitation Spectra and the UV−Visible Absorption Spectra: Intramolecular Energy Transfer. In order to study the intramolecular singlet energy transfer, the fluorescence excitation spectra of **B-1** and **B-2** were compared with the UV−vis absorption spectra (Figure 7).[55] It is unreliable to evaluate the intramolecular energy transfer by using the quenching of the fluorescence of the energy donor,[61] although this method was very often used. Singlet energy transfer is not the only factor that contributes to the quenching of the fluorescence, electron

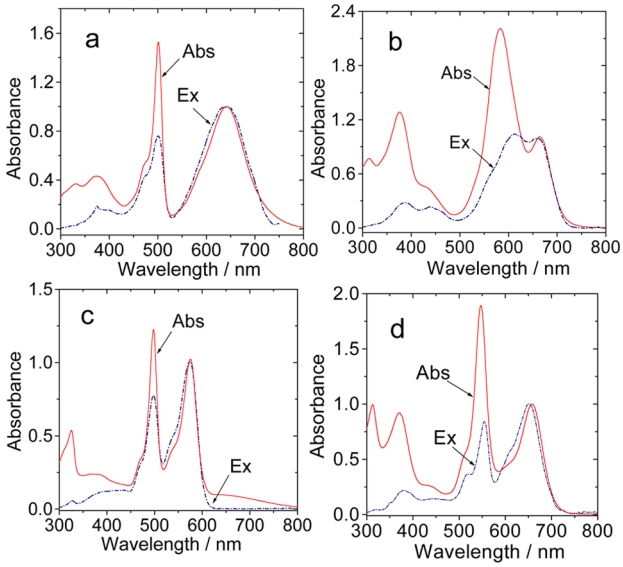

Figure 7. Comparison of the fluorescence excitation and UV−vis absorption spectra. (a) **B-1** (λ_{em} = 750 nm for the excitation spectrum) and (b) **B-2** (λ_{em} = 700 nm). $c = 1.0 \times 10^{-5}$ M in CH_2Cl_2. (c) **B-1** (λ_{em} = 593 nm) and (d) **B-2** (λ_{em} = 700 nm). $c = 1.0 \times 10^{-5}$ M in MeCN/H_2O = 9:1 (v/v) and 100 μL of 1 M HCl was added. 20 °C. The unprotonated **B-1** and **B-2** are nonfluorescent in aqueous solution, thus CH_2Cl_2 was used for measuring the excitation spectra in the absence of acid (trifluoroacetic acid).

transfer may be also responsible for the quenching of the fluorescence of the energy donor. For **B-1**, upon normalization of the UV−vis absorption and the fluorescence excitation spectra at 575 nm, the excitation band at 499 nm is relatively weaker than the UV−vis absorption band at the same position (Figure 7a). The intramolecular energy transfer was calculated as 66%.[55] Similar intramolecular energy transfer efficiency (46%) was observed for **B-2** (Figure 7b).

dx.doi.org/10.1021/jo5019014 | J. Org. Chem. 2014, 79, 10240−10255

Upon protonation, the absorption bands of the dimethylamino styryl-Bodipy parts in both **B-1** and **B-2** are blue-shifted (Figure 7c,d). However, similar intramolecular energy transfer efficiency were observed compared with that of the neutral form of the compounds. The unprotonated **B-1** and **B-2** are nonfluorescent in aqueous solution, thus CH_2Cl_2 was used for measuring the excitation spectra of the compounds in the absence of acid (trifluoroacetic acid, TFA). Moreover, the excitation spectra of **B-2** in polar solvents such as methanol and acetonitrile were also studied (Supporting Information, Figure S22), and the results show that the excitation at ~580 nm disappeared in polar solvents. This observation is in agreement with the postulation that in polar solvents the component absorbing at shorter wavelength in **B-2** transformed into a singlet energy acceptor in the FRET process (Figure 3).

The luminescence lifetimes of the dyads and the reference compounds in solvents with different polarity were also studied (Table 2). Because of the intramolecular charge transfer feature

Table 2. Luminescent Lifetimes of B-1− B-4 under Different Conditions[a]

	toluene	CH_2Cl_2	CH_3CN	no acid/base	with acid	with base
B-1	1.90	1.12	–[b]	–[b]	0.52	–[b]
B-2	1.72	1.46	1.19	1.15	1.56	–[b]
B-3	1.94	1.55	–[b]	–[b]	0.59	–[b]
B-4	2.14	2.13	2.13	1.98	2.01	–[b]
4	3.84	3.66	1.29	0.87	4.11	0.80

[a]In ns. c = 1.0 × 10^{-5} M, 20 °C. [b]Too weak to be determined accurately.

of the emissive parts in **B-1** and **B-3**, the fluorescence lifetime becomes shorter with the solvents switched from toluene to acetonitrile. For example, the fluorescence lifetime is 1.90 ns for **B-1** in toluene, but the fluorescence was not observed in CH_3CN. With the amino group protonated, the fluorescence lifetime was observed as 0.52 ns. **B-3** shows similar properties. The ICT effect of reference **4** is significant, so with solvent polarity increased, the fluorescence lifetime becomes shorter. **B-2** gives a fluorescence lifetime of 1.72 ns in toluene, but this values was reduced to 1.19 ns in CH_3CN. With the amino group protonation, the ability of the ICT property of reference compound **4** disappeared, as a result fluorescence lifetime is prolonged.

2.5. Nanosecond Transient Absorption Spectroscopy: Switching of the Triplet Excited State Upon Protonation. Previously, the effect of solvent polarity and pH on UV−vis absorption and fluorescence of dimethylamino styryl Bodipy was studied, but the same effect on the triplet excited states were not studied with nanosecond time-resolved transient absorption spectroscopy.[59a] Herein the triplet excited states of the compounds were studied with nanosecond time-resolved transient difference absorption spectroscopy (Figure 8). For neutral **B-1** in toluene, the bleaching band at 650 nm was observed upon 532 nm nanosecond pulsed laser excitation (Figure 8a). Transient absorption band in the 700−850 nm region with a lifetime of 4.0 μs was observed. These features are in agreement with a previous study on the triplet state of diiodostyrylBodipy.[60] As no bleaching band at 490 nm was found, therefore, the triplet excited state of **B-1** (in toluene) is localized on the diiodostyryl Bodipy part, not on the Bodipy part. No transient absorption can be observed for **B-1** in

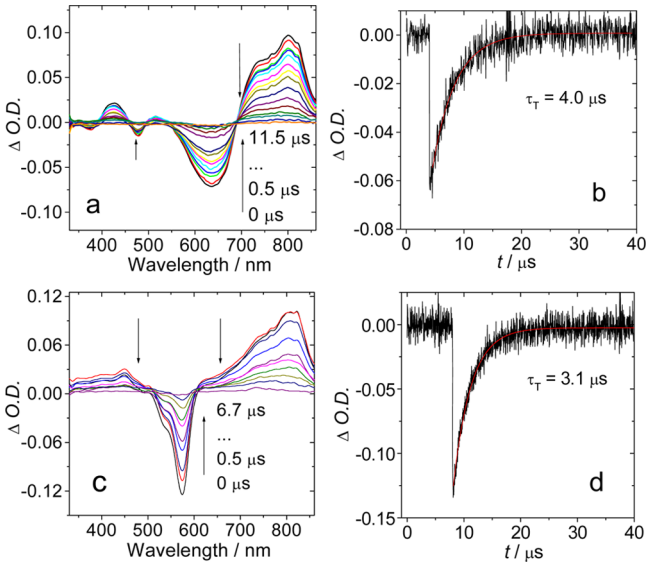

Figure 8. (a) Nanosecond time-resolved transient difference absorption spectra of **B-1** and (b) decay trace of **B-1** at 620 nm (in toluene); (c) transient absorption difference spectra and (d) the decay trace at 580 nm (in deaerated MeCN/H_2O = 9:1 (v/v) with 100 μL of 1 M HCl added). λ_{ex} = 532 nm, c = 1.0 × 10^{-5} M, 20 °C.

solvents with higher polarity, such as CH_2Cl_2 and MeCN/H_2O (9:1, v/v).

Upon addition of HCl to the solution of **B-1** in MeCN/H_2O (9:1, v/v), however, transient spectra with a significant bleaching band at 580 nm (Figure 8c,d, τ_T = 3.1 μs) were observed. This bleaching band is attributed to the depletion of the ground state of the protonated iodo- dimethylaminostyryl Bodipy part, based on the steady state UV−vis absorption spectra of **B-1** upon protonation (Figure 5a). By comparison with the reference **B-3** (Figure S29 in the Supporting Information), we conclude that the T_1 state of protonated **B-1** is localized on the iodo-dimethylamino styryl Bodipy part, not on the unsubstituted Bodipy part. Thus, the triplet excited state in **B-1** can be switched ON with protonation. We noted the triplet state lifetime of **B-1** is slightly shorter than the reference compound **B-3** (τ_T = 6.6 μs).

The nanosecond transient absorption spectra of **B-2** in toluene were studied (Figure 9a). The bleaching band at 660 nm was observed, which is assigned to the depletion of the ground state of the iodo-styryl Bodipy part in **B-2**. Transition absorption band at 417, 551, and 760 nm were observed. By comparison with the TA spectra of **B-4** (Figure 9e), the T_1 state of **B-2** is assigned to the iodo-styryl Bodipy moiety. A minor bleaching band at 594 nm was observed, which is due to the 4′-dimethylamino styryl Bodipy moiety. By comparison with the steady state UV−vis absorption of **B-2**, we propose there is a triplet state equilibrium for **B-2**, with the triplet excited state localized more significantly on the iodo-styryl Bodipy moiety.

Note in polar solvents, such as CH_2Cl_2 and MeCN/H_2O (9:1, v/v), no transient signal was detected for the neutral form of **B-2**. The lack of the triplet state may be due to the low-lying T_1 state on the 4′-dimethylamino styryl Bodipy part, for which the T_1 state was quenched by the ICT effect. This is confirmed by the study of the TA spectra of **B-3** in different solvents. In toluene, triplet excited states were observed with lifetimes of 4.4 μs (see the Supporting Information, Figure S31). In polar

dx.doi.org/10.1021/jo5019014 | J. Org. Chem. 2014, 79, 10240−10255

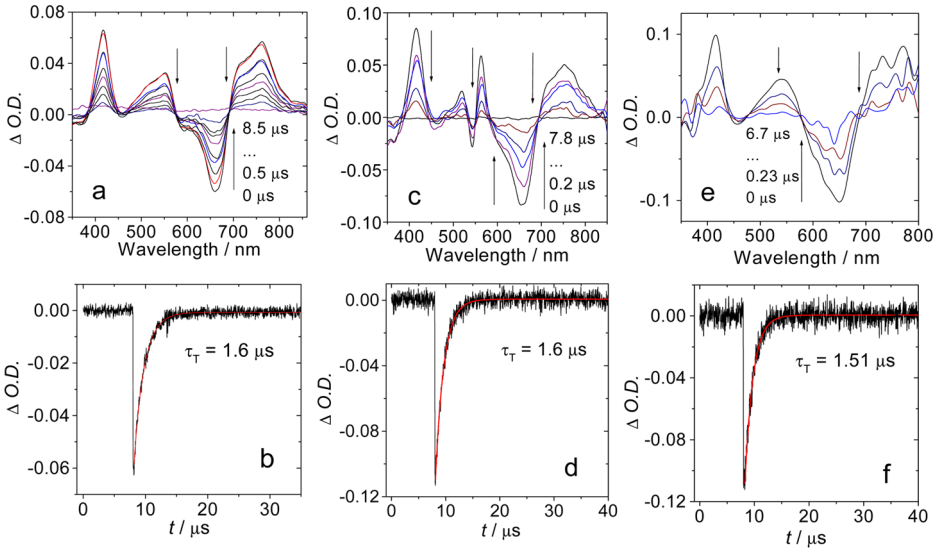

Figure 9. Nanosecond time-resolved transient difference absorption spectra of (a) **B-2** and (b) decay trace of **B-2** at 660 nm (in toluene); (c) **B-2** and (d) decay trace of **B-2** at 660 nm. (e) **B-4** and (f) decay trace of **B-4** at 660 nm. For samples in parts c–f, the solution of deaerated MeCN/H_2O = 9:1 (v/v) was used (with 100 μL of 1 M HCl added). λ_{ex} = 532 nm, c = 1.0 × 10^{-5} M, 20 °C.

solvents such as CH_2Cl_2 and MeCN/H_2O (9:1, v/v), no transient signal can be detected for **B-3**. Signal was observed only in the presence of acid (Figure S29 in the Supporting Information).

Note the dimethylaminostyryl Bodipy moiety in **B-2** is the singlet energy acceptor, but the triplet state of energy donor in **B-2** can still be populated, which means that the ISC was not completely inhibited by the FRET. This finding is different from a previous study.[33a]

Upon protonation in MeCN/H_2O (9:1, v/v), transient bands were observed for **B-2** (Figure 9c). A minor bleaching band at 542 nm and a major bleaching band at 654 nm were observed, which decay uniformly (1.6 μs). These bands corresponded to the steady state UV–vis absorption of the protonated 4′-dimethylamino styryl Bodipy moiety and the iodo-styryl Bodipy parts in **B-2** (Figure 6a), respectively. Therefore, the triplet excited state of **B-2** is *delocalized* on the protonated dimethylaminostyryl Bodipy part and the 4-hydroxyl styryl Bodipy parts, i.e., there is a triplet state equilibrium.[40] On the basis of the steady state molar absorption coefficients of the two absorption bands (Figure 6a), we propose that the triplet state is more localized on the iodinated styrylBodipy part than on the protonated dimethylamino styryl Bodipy part.[40]

The triplet state equilibrium in **B-2** was supported by the nanosecond transient absorption spectra of the reference **B-4**, for which a transient bleaching band at 654 nm was detected, but there is no bleaching band at 542 nm (Figure 9e, Table 3). Note the absorption band in the 500–600 nm was distorted in **B-2**, due to the bleaching band (with negative O.D. values) at 542 nm. The presence of triplet state equilibrium in protonated **B-2** is also supported by the DFT calculations on the triplet excited state energy levels, which indicated that there are two *degenerated* low-lying triplet states (T_1 and T_2 states, with energy levels of 1.08 and 1.26 eV, respectively), which are localized on the dimethylamino styryl Bodipy part and the 4-hydroxyl styryl Bodipy part, respectively (see later section).

For the neutral form of **B-2** in MeCN/H_2O (9:1, v/v), we propose that the T_1 state is localized on the dimethylamino styryl Bodipy part, thus no long-lived transient can be detected due to the significant ICT effect of the dimethylamino styryl Bodipy part (similar to **B-3**). Upon protonation, the energy level of the dimethylamino styryl Bodipy part in **B-2** increased and the triplet state is localized on the energetically low-lying 4-hydroxyl styryl Bodipy part. Such a shuffling of the localization of the triplet excited state in a chromophore dyad with external stimuli was not reported. Switching of the triplet excited states of organic chromophore dyads may offer a new method to construct complicated functional molecular arrays, such as molecular logic gates, or switchable PDT reagents.

Table 3. Photophysical Parameters of the Compounds in the Presence of Acid (HCl)[a]

	λ_{abs} (nm)	ε/ 10^5 M^{-1} cm^{-1}	λ_{em} (nm)	Φ_L[b] (%)	τ_T[c] (μs)	τ_F[d] (ns)
B-1	497/575	0.94/0.80	509/594	3.69	3.1	0.47
B-2	552/663	1.12/0.59	564/693	1.02	1.6	1.54
B-3	575	0.81	593	2.54	6.6	0.53
B-4	654	0.83	689	5.0	1.5	2.16
4	556	1.12	565	71	–	4.11

[a]Recorded CH_3CN/H_2O (9/1, v/v) with 100 μL HCl (1.0 M) added. 20 °C. [b]Fluorescence quantum yield. [c]Triplet excited state lifetimes. Measured by nanosecond transient absorption in deaerated solutions. [d]Luminescent lifetimes, λ_{ex} = 472.6 nm (pulsed laser).

2.6. DFT Calculations on the Photophysical Properties of the Triplet Photosensitizers. The geometries of dyad **B-1** at the ground state was optimized with the DFT method.[40,53,62−65] An extended geometry was found for **B-1**, i.e., the energy donor and acceptor are far away from each other.

The excitation energy for the singlet and triplet excited states of **B-1** were computed with the TD-DFT method. The electronic transitions (Table 4) and the molecular orbitals were analyzed (Scheme 2). Highest occupied molecular orbital (HOMO) and lowest unoccupied molecular orbital (LUMO) are involved in the $S_0 \rightarrow S_1$ transition. Both MOs are localized on the styryl-iodo Bodipy moiety. The calculated absorption wavelength is 630 nm, which is in agreement with the experimental value of the UV–vis absorption of **B-1** (639 nm, Figure 1a). HOMO−1 → LUMO+1 are involved in the S_2

dx.doi.org/10.1021/jo5019014 | J. Org. Chem. 2014, 79, 10240−10255

Table 4. Selected Parameters for the Calculated UV−Visible Absorption and Triplet State Energy level of the Compound B-1[a]

TDDFT/B3LYP/6-31G(d)/LANL2DZ				
electronic transition[b]	excitation energy	f[c]	composition[d]	CI[e]
$S_0 \rightarrow S_1$	1.97 eV (630 nm)	1.0911	H → L	0.7088
$S_0 \rightarrow S_2$	2.90 eV (426 nm)	0.5862	H−1 → L+1	0.6993
$S_0 \rightarrow S_{15}$	3.64 eV (341 nm)	0.6275	H → L+2	0.5903
$S_0 \rightarrow T_1$	1.14 eV (1083 nm)	0.0000	H → L	0.6690
		0.0000	H−2 → L	0.2214
$S_0 \rightarrow T_2$	1.54 eV (807 nm)	0.0000	H−1 → L+1	0.7101
$S_0 \rightarrow T_3$	2.04 eV (608 nm)	0.0000	H−2→ L+1	0.6379

[a]Electronic excitation energies (eV) and oscillator strengths (f), configurations of the low-lying excited states of **B-1**. Calculated by TDDFT/B3LYP/6-31G(d)/LANL2DZ, based on the optimized ground-state geometries (CH_3CN was used as solvent). [b]Only selected excited states were considered. Numbers in parentheses are the excitation wavelength. [c]Oscillator strength. [d]H stands for HOMO and L stands for LUMO. Only the main configurations are presented. [e]Coefficient of the wave function for each transition. CI coefficients are in absolute values.

state. The predicated absorption wavelength is 426 nm. The discrepancy between the calculated value and the experimental value is within expectation because it is known that the UV−vis absorption of the unsubstituted Bodipy cannot be predictably precisely with the DFT method. The triplet excited states of **B-1** were also studied with TDDFT calculations based on the optimized ground state geometry (Table 4). The T_1 state is localized on the styryl iodo-Bodipy part, the T_2 state is localized on the Bodipy part, for which the calculated energy level is 1.54 eV. This value is close to the experimental results (1.70 eV).[60b] Because of the large energy gap (0.4 eV) between the T_1 and the T_2 state, no excited state equilibrium should be observed.[40] This postulation is consistent with the nanosecond transient absorption spectroscopy.

The excitation and the triplet state of the *protonated* **B-1** was also studied (Scheme 3 and Table 5). The S_1 state is a charge transfer state. Two absorption bands at 512 and 426 nm were predicted by the TDDFT method. The blue shift of the transition localized on the iodo-styryl Bodipy part is in agreement with the experimental results. The triplet excited states of the protonated **B-1** were also studied with the TDDFT method. The T_1 state is localized on the styryl-iodo Bodipy part, and the T_2 state is localized on the Bodipy part. The energy gap is 0.2 eV.

A similar calculation was applied to **B-2** (Scheme 4 and Table 6). Two major absorption bands at 636 and 584 nm were found, which are in good agreement with the experimental results (660 and 589 nm, Figure 2a). These two absorption bands are attributed to the diiodo-styryl Bodipy and the 4′-dimethylamino styryl Bodipy moiety of **B-2**, respectively, based on the transitions involved in the excitations HOMO−1 → LUMO and HOMO → LUMO+1 (Scheme 4).

The triplet excited states were also studied with the TDDFT calculations. The T_1 state is localized on the diiodo-styryl Bodipy part, with energy level of 1.09 eV. The T_2 state is localized on the 4′-dimethylamino styryl Bodipy part, with an energy level of 1.16 eV. The similar energy level indicated that triplet state equilibrium is possible. This postulation is in agreement with the nanosecond time-resolved transient absorption spectra of **B-2** in toluene (Figure 8a), in which both bleaching bands corresponding to both Bodipy moieties were found.

Similar DFT/TDDFT calculations were applied to the protonated **B-2** (Scheme 5 and Table 7). The absorption band at 636 nm is assigned to the diiodo-styryl Bodipy part in **B-2**. The calculated absorption wavelength is similar to that at neutral conditions. This finding is in agreement with the experimental results. An absorption band at 509 nm was also

Scheme 2. Selected Frontier Molecular Orbitals Involved in the Excitation, and Triplet Excited States of B-1[a]

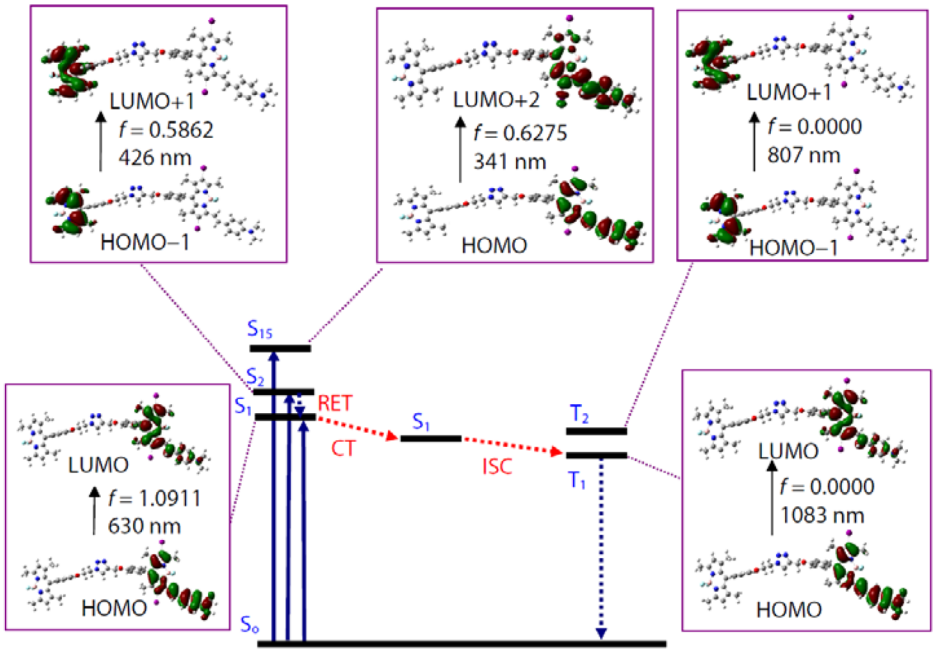

[a]CH_3CN was used as solvent in the calculation. CT stands for conformation transformation.

dx.doi.org/10.1021/jo5019014 | J. Org. Chem. 2014, 79, 10240−10255

Scheme 3. Selected Frontier Molecular Orbitals Involved in the Excitation and Triplet Excited States of B-1 in the Presence of Acid[a]

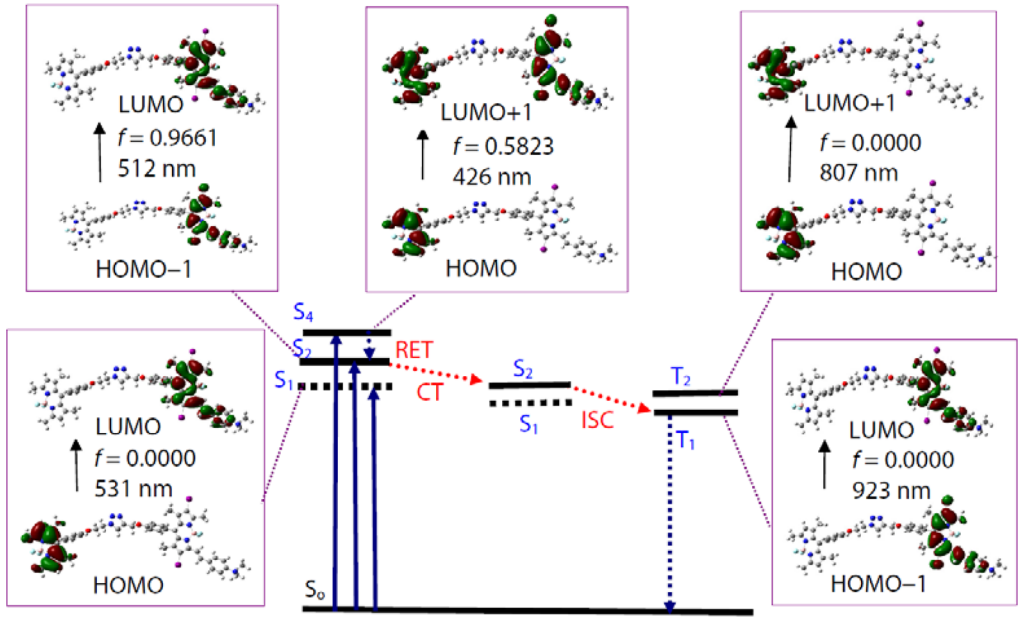

[a]CH_3CN was used as solvent in the calculation. CT stands for conformation transformation.

Table 5. Selected Parameters for the Calculated UV−Visible Absorption of the Protonated Compound B-1[a]

TDDFT/B3LYP/6-31G(d)/LANL2DZ				
electronic transition[b]	excitation energy	f[c]	composition[d]	CI[e]
$S_0 \rightarrow S_1$	2.33 eV (531 nm)	0.0000	H → L	0.7088
$S_0 \rightarrow S_2$	2.39 eV (512 nm)	0.9661	H−1 → L+1	0.6993
$S_0 \rightarrow S_4$	2.91 eV (426 nm)	0.5823	H → L+2	0.5903
$S_0 \rightarrow T_1$	1.33 eV (928 nm)	0.0000	H → L	0.6690
$S_0 \rightarrow T_2$	1.53 eV (807 nm)	0.0000	H−2 → L	0.2214

[a]Electronic excitation energies (eV) and oscillator strengths (f) of the low-lying excited states of **B-1** added acid. Calculated by TDDFT/B3LYP/6-31G(d)/LANL2DZ, based on the optimized ground-state geometries (CH_3CN was used as solvent in the calculation). [b]Only selected excited states were considered. Numbers in parentheses are the excitation wavelength. [c]Oscillator strength. [d]H stands for HOMO and L stands for LUMO. Only the main configurations are presented. [e]Coefficient of the wave function for each transition. CI coefficients are in absolute values.

predicted by the TDDFT calculation, which is blue-shifted as compared with the TDDFT results of the neutral form **B-2** (Table 3). The T_1 state is identified as a triplet state localized on the diiodo-styryl Bodipy, and the T_2 state is localized on the 4′dimethylamino styryl Bodipy. The small energy gap of the T_1 and T_2 state indicates that triplet state equilibrium is possible.

2.7. Electrochemical Studies. In order to study the photoinduced intramolecular electron transfer in the dyads, the electrochemistry of **B-1**, reference **B-3**, and Bodipy were studied by using cyclic voltammetry (CV) in CH_2Cl_2 (Figure 10 and Table 8. For **B-2**, **B-4** and **4**, see Figure S57 in the Supporting Information and Table 8). For **B-3**, there are two reversible oxidation potential at +0.41 V, +0.78, and one reversible reduction potential at −1.16 V. Bodipy shows reversible oxidation and reduction potentials at +0.92 V, −1.54 V. For **B-1**, in the anodic scan, it exhibits three irreversible oxidization peaks at around +0.58 V, +0.91 V, and +1.06 V, respectively. The first oxidation comes from 4-*N*,*N*-dimethylamino styryl Bodipy (+0.58 V, +0.91 V) and the second oxidation process lies in Bodipy (+1.06 V). In the cathodic scanning, **B-1** also reveals an electrochemically irreversible process.

The first reduction wave is due to 4-*N*,*N*-dimethylamino styrylBodipy (−1.07 V), and the second reduction wave is from Bodipy unit (−1.38 V) compared with the reference compounds **B-3** and Bodipy. The Gibbs free energy was calculated by the Rehm−Weller equation for the **B-1** diiodo styryl Bodipy part as an electron donor that corresponds to the Bodipy moiety as an electron acceptor. For **B-2**, the dimethylaminostyryl Bodipy part acts as an electron donor and the hydroxyl styryl Bodipy moiety is as electron acceptor. $\Delta E_{0,0}$ is the singlet excited state level (for the calculation process, see the Supporting Information). **B-1** (ΔG_{ET} = +0.09 eV) and **B-2** (ΔG_{ET} = −0.70 eV). On the basis of the analysis of the ΔE_{ET} values, the driving force of intramolecular charge transfer in **B-2** is thermodynamically allowed.[24,40,58,66,67]

The photophysical process of **B-1** are summarized in Scheme 6. In the neutral form, the fluorescence of the Bodipy part in **B-1** is efficiently quenched by the FRET to the iodostyrylBodipy part. The T_1 state of the unsubstituted Bodipy is with higher energy level than the T_1 state of the 2,6-diiodo styryl Bodipy, and the ISC of the unsubstituted Bodipy is very weak. The singlet excited state and the triplet excited state of the iodo-styryl Bodipy part were efficiently quenched by the charge transfer (ICT). As a result, no fluorescence and long-lived triplet excited state can be observed for **B-1**. These postulations were confirmed by the steady state and the nanosecond time-resolved transient difference absorption spectra of **B-1**. It should be pointed out that quenching of the triplet excited state of the organic chromophore by the photoinduced charge

dx.doi.org/10.1021/jo5019014 | J. Org. Chem. 2014, 79, 10240−10255

Scheme 4. Selected Frontier Molecular Orbitals Involved in the Excitation, Emission, and Triplet Excited States of B-2[a]

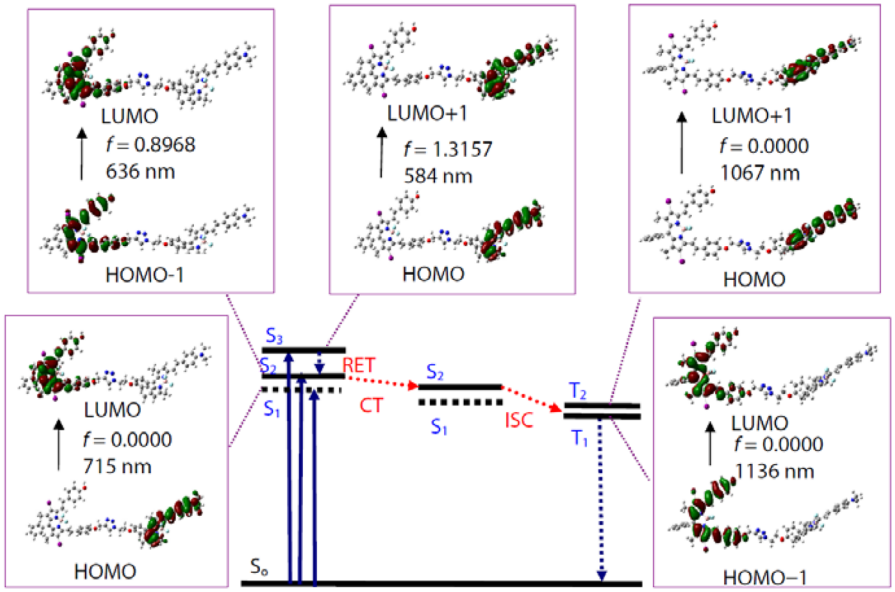

[a]CH_3CN was used as solvent in the calculation. CT stands for conformation transformation.

Table 6. Selected Parameters for the Calculated UV−Visible Absorption and Triplet State Energy Level of B-2[a]

TDDFT/B3LYP/6-31G(d)/LANL2DZ				
electronic transition[b]	excitation energy	f[c]	composition[d]	CI[e]
$S_0 \rightarrow S_1$	1.73 eV (715 nm)	0.0000	H → L	0.7070
$S_0 \rightarrow S_2$	1.95 eV (636 nm)	0.8968	H−1 → L	0.7076
$S_0 \rightarrow S_3$	2.12 eV (584 nm)	1.3157	H → L+1	0.7083
$S_0 \rightarrow T_1$	1.09 eV (1136 nm)	0.0000	H−1 → L	0.6960
$S_0 \rightarrow T_2$	1.16 eV (1067 nm)	0.0000	H → L+1	0.6769
$S_0 \rightarrow T_3$	1.73 eV (715 nm)	0.0000	H → L	0.7070

[a]Excitation energies (eV) and oscillator strengths (f) of the states of **B-2**. Calculated by TDDFT/B3LYP/6-31G(d)/LANL2DZ, based on the optimized ground-state geometries (CH_3CN was used as solvent). [b]Only selected excited states were considered. Numbers in parentheses are the excitation wavelength. [c]Oscillator strength. [d]H stands for HOMO and L stands for LUMO. Only the main configurations are presented. [e]Coefficient of the wave function for each transition. CI coefficients are in absolute values.

transfer (ICT) mechanism was not reported. Previously the quenching mechanism is based on either PET or FRET.[7,33,34] Our results will shed a light on new approaches to switch the triplet excited states of organic chromophores. Upon protonation, RET still exists even with the blue-shifted absorption of the dimethylaminostyryl Bodipy part. However, long-lived triplet excited state was observed due to the elimination of the ICT effect.

The photophysical property of **B-2** was summarized in Scheme 7. In order to explain the photophysical process, the large Stokes shift of the dimethylaminostyryl Bodipy part must be considered. This part gives shorter absorption wavelength; however, its emission wavelength is longer than the hydroxyl styryl Bodipy part, especially in polar solvents. As a result, the fluorescence of the hydroxylstyryl Bodipy part is substantially quenched by the FRET with the dimethylamino styryl Bodipy part as the energy acceptor. The latter is known for its nonfluorescent feature in polar solvents, due to ICT. This is a rare example for which the energy acceptor gives shorter absorption wavelength than the energy donor in a FRET dyad. The triplet state of the hydroxyl styryl Bodipy part is quenched by the triplet−triplet-energy-transfer to the dimethylamino styryl Bodipy part, and the latter is quenched by the ICT effect. As a result, no long-lived triplet excited state was observed for **B-2** upon photoexcitation.[33]

Upon protonation of the dimethylamino group, the charge transfer state (CTS) will disappear, the S_1 state energy level and the T_1 state energy level of the dimethylamino styryl Bodipy part will increase. These changes of the excited state of the dimethylamino styryl Bodipy part will impart substantial influence on the overall photophysical property of **B-2**, i.e., there will be a "switching" effect upon protonation. First, the FRET from the hydroxyl styryl Bodipy part to the dimethylamino styryl Bodipy part is reduced, as a result, the fluorescence of the hydroxyl styryl Bodipy part is enhanced. Note the fluorescence is still weak because of the heavy atom effect of the iodo- atoms attached on this part of the dyad. Second, the triplet state energy level of the dimethylamino styryl Bodipy part is presumably increased upon protonation; as a result, equilibrium between the triplet state of the hydroxyl styryl Bodipy part and the dimethylamino styryl Bodipy part was observed with the nanosecond time-resolved transient difference absorption spectra. This is different from **B-1** in which the two components show a drastically different T_1 state energy level; as a result, no triplet state equilibrium was observed for **B-1** upon protonation.

2.8. Switching of the Singlet Oxygen ($^1O_2$) Production by Protonation. The application potential of the triplet photosensitizers in photosensitizing is highly dependent on the property of the triplet state. In order to monitor the singlet oxygen ($^1O_2$) production kinetics, 1,3-diphenylisobenzofuran (DPBF) was used as a $^1O_2$ scavenger.[68] The $^1O_2$ photosensitizing of the triplet photosensitizers in the absence and presence of acid were studied (Figure 11). For **B-1**, no $^1O_2$ can be detected upon photoirradiation at 592 nm. Upon addition of HCl, significant $^1O_2$ production upon photoexcitation was

dx.doi.org/10.1021/jo5019014 | J. Org. Chem. 2014, 79, 10240−10255

Scheme 5. Selected Frontier Molecular Orbitals Involved in the Excitation, Emission, and Triplet Excited States of B-2 With Acid Added[a]

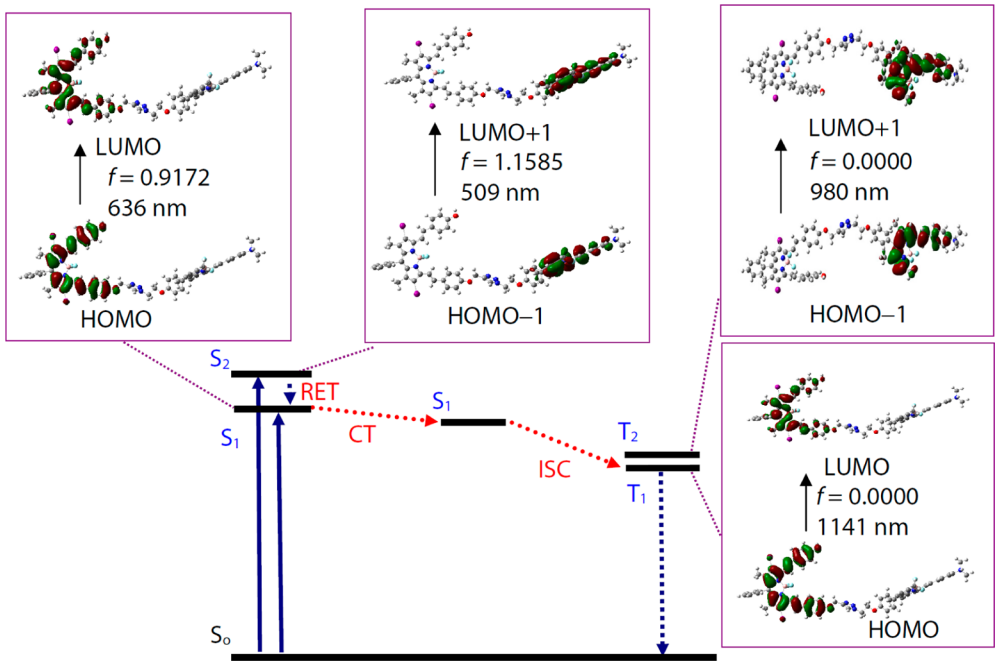

[a]CT stands for conformation transformation.

Table 7. Selected Parameters for the Calculated UV−Visible Absorption and Triplet Excited States of the Protonated B-2[a]

TDDFT/B3LYP/6-31G(d)/LANL2DZ				
electronic transition[b]	excitation energy	f[c]	composition[d]	CI[e]
$S_0 \rightarrow S_1$	1.95 eV (636 nm)	0.9172	H → L	0.7079
$S_0 \rightarrow S_2$	2.44 eV (509 nm)	1.1585	H−1 → L+1	0.7072
$S_0 \rightarrow S_3$	2.61 eV (474 nm)	0.4937	H−1 → L	0.6905
$S_0 \rightarrow T_1$	1.08 eV (1141 nm)	0.0000	H → L	0.6965
$S_0 \rightarrow T_2$	1.26 eV (980 nm)	0.0000	H−1 → L+1	0.7069

[a]Electronic excitation energies (eV) and oscillator strengths (f), configurations of the low-lying excited states of **B-2**. Calculated by TDDFT/B3LYP/6-31G(d)/LANL2DZ, based on the optimized ground-state geometries (CH_3CN was used as solvent in the calculation). [b]Only selected excited states were considered. Numbers in parentheses are the excitation wavelength. [c]Oscillator strength. [d]H stands for HOMO and L stands for LUMO. Only the main configurations are presented. [e]Coefficient of the wave function for each transition. CI coefficients are in absolute values

observed, indicated by the decreasing of the absorbance of DPBF at 414 nm. The $^1O_2$ quantum yield was determined as 6.9% and 69.0% for the neutral and the protonated form of **B-1**. Thus, the $^1O_2$ production with **B-1** can be activated by addition of acid. Similar results were observed for **B-2** and **B-3** (Figure 11e,d). For **B-4**, however, similar $^1O_2$ photosensitizing ability was found under neutral and acid condition, indicating that the triplet state of the 2,6-diiodo-4-hydroxylstyryl Bodipy was not affect by the presence of acid.

4-Hydroxylphenyl styryl 2,6-diiodo-Bodipy is sensitive to KOH due to the hydroxylphenyl group.[69] For the UV−vis absorption of **B-2**, with addition of KOH, a new absorption band at 734 nm developed and the absorption band at 660 nm decreased (Figure S20 in the Supporting Information) Fluorescence intensity of **B-2** at 693 nm is also decreased with the addition of KOH (Figure S20 in the Supporting Information). Similar results were found for **B-4** (Figure S21 in the Supporting Information). The ability of $^1O_2$ production by **B-2** and **B-4** was also investigated in the presence of KOH. For **B-4**, the singlet oxygen quantum yield is high (52.7%), but no $^1O_2$ was produced in the presence of KOH (Figures S46, S47, S50, and S51 in the Supporting Information).

The production of $^1O_2$ can be used for organic synthesis purpose. For example, 1,5-dihydroxylnaphtalene can be oxidized by $^1O_2$ to produce juglone. Juglone can be used for preparation of bioactive compounds. The results show that the photooxidation of DHN proceeded smoothly. The photooxidation can also be switched by acid. For example, the production of juglone in the absence of aqueous HCl is negligible for **B-1** and **B-2**.

With addition of aqueous HCl, production of juglone upon photooxidation of DHN is significant. The $^1O_2$ quantum yields (Φ_Δ) of the compounds in the absence and in the presence of aqueous HCl were compared. For example, **B-1** gives a Φ_Δ value of 6.9% in the absence of aqueous HCl. In the presence of aqueous HCl, the Φ_Δ value increased by 10-fold to 69% (Table 9. For the results of **B-3** and **B-4**, see the Supporting Information, Figures S38 and S39).

2.9. Conclusions. In conclusion, two Bodipy-derived dyads were prepared. We demonstrated that the *triplet* excited state of 2,6-diiodo-4′-dimethylaminostyryl-Bodipy can be switched ON by protonation of the amino group. In the neutral form, nanosecond transient absorption spectra show that the excited state is short-lived (<10 ns) and no singlet oxygen ($^1O_2$) can be

dx.doi.org/10.1021/jo5019014 | J. Org. Chem. 2014, 79, 10240−10255

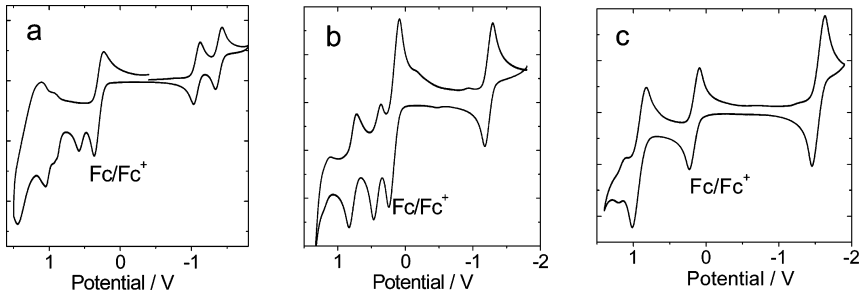

Figure 10. Cyclic voltammogram of (a) **B-1**, (b) **B-3**, and (c) Bodipy. Ferrocene (Fc) was used as internal reference ($E_{1/2}$ = +0.64, Fc^+/Fc) vs standard hydrogen electrode). In deaerated CH_2Cl_2 solutions containing 1.0 mM **B-1** alone, or with the ferrocene, 0.10 M Bu_4NPF_6 as supporting electrode, $Ag/AgNO_3$ reference electrode. Scan rates: 0.1 V/s.

Table 8. Redox Potentials of Bodipy Photosensitizers for Study of the Potential Intramolecular Electron Transfer by the Estimation of Free-Energy Changes for the Charge Separation ΔG_{ET} (Photoinduced Electron Transfer)[a]

	E(Ox) (V)	E(Red) (V)	ΔG_{ET}[b] (eV)
4	+0.34, +0.65	−1.46	–
Bodipy	+0.92	−1.54	–
B-1	+0.58, +0.91, +1.06	−1.07, −1.38	+0.58[c]/+0.09[d]
B-2	+0.29, +0.67	−0.83, −1.03	−0.05[c]/−0.70[d]
B-3	+0.41, +0.78	−1.16	–
B-4	+0.67, +0.95	−1.08	–

[a]Anodic and cathodic peak potential were presented. The potential values of the compounds are vs saturated calomel electrode. Cyclic voltammetry in N_2 saturated CH_2Cl_2 containing a 0.10 M Bu_4NPF_6 supporting electrolyte; counter electrode is Pt electrode; working electrode is glassy carbon electrode; $Ag/AgNO_3$ couple as the reference electrode. c [Ag^+] = 0.1 M. 1.0 mM dyad photosensitizers in CH_2Cl_2, 20 °C. Conditions: 1.0 mM dyad photosensitizers and 1.0 mM ferrocene in CH_2Cl_2, 25 °C and calculate relative to the SCE (saturated calomel electrode). [b]ΔG_{ET} is the free energy changes of the intramolecular electron transfer, with dimethylamino styrylBodipy as the electron donor. [c]Via triplet state. [d]Via singlet state. For details, refer to the Supporting Information.

produced, thus the triplet state is OFF. Upon protonation, however, a long-lived triplet excited state was observed (τ_T = 6.6 μs) and photosensitizing of $^1O_2$ was observed (Φ_Δ = 79.8%). A similar switching effect was also observed in polar and nonpolar solvents such as dichloromethane and toluene. Tuning of the energy levels of the components of the dyads were utilized to switch the triplet excited state property, supported by the steady state and time-resolved absorption and fluorescence emission spectroscopy. The switching of the triplet excited state of 2,6-diiodo-4′-dimethylaminostyryl-Bodipy was demonstrated in two Bodipy dyads which show broadband visible light absorption. Interestingly the triplet excited state of one dyad is *delocalized* on both of the Bodipy units, i.e., there is a triplet excited state equilibrium. Moreover, we observed a rare example that the singlet energy acceptor of the fluorescence-resonance-energy-transfer (FRET) gives shorter absorption wavelength than the energy donor. We also show that the ISC cannot be inhibited by the competing FRET effect. The experimental results were rationalized by DFT and time-dependent DFT (TDDFT) calculations. The switching of the triplet excited states of the dyads was transduced in the $^1O_2$ photosensitizing with the dyads as a triplet photosensitizer. These detailed investigations on the switching of triplet excited states of organic chromophore dyads, especially with nanosecond time-resolved transient difference absorption spectroscopy, may offer new approaches for designing molecular assemblies with sophisticated switchable functionalities.

3. EXPERIMENTAL SECTION

3.1. Compounds **1**, **3**, and **5** were synthesized according to literature methods.[40]

3.2. Synthesis of 2. A mixture of compound **1** (126.6 mg, 0.2 mmol) and 4-*N*,*N*-dimethylbenzaldehyde (124 mg, 0.8 mmol) was dissolved in dry toluene (20 mL), then 0.2 mL acetic acid and 0.2 mL piperidine were added under Ar. The mixture was refluxed for 4 h. After completion of the reaction, the reaction mixture was cooled to

Scheme 6. Simplified Jablonski Diagram Illustrating the Photophysical Processes Involved in (a) B-1 in the Absence of Acid and (b) B-1 in the Presence of Acid[a]

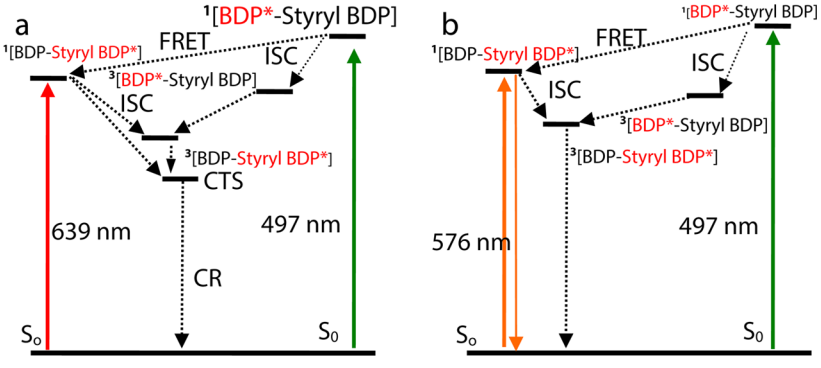

[a][BDP-Styryl Bodipy] stands for **B-1**. The component at the excited state was designated with red color and a asterisk. The number of the superscript designated either the singlet or the triplet excited state.

dx.doi.org/10.1021/jo5019014 | J. Org. Chem. 2014, 79, 10240−10255

Scheme 7. Simplified Jablonski Diagram Illustrating the Photophysical Processes Involved in (a) B-2 in the Absence of Acid and (b) B-2 in the Presence of Acid[a]

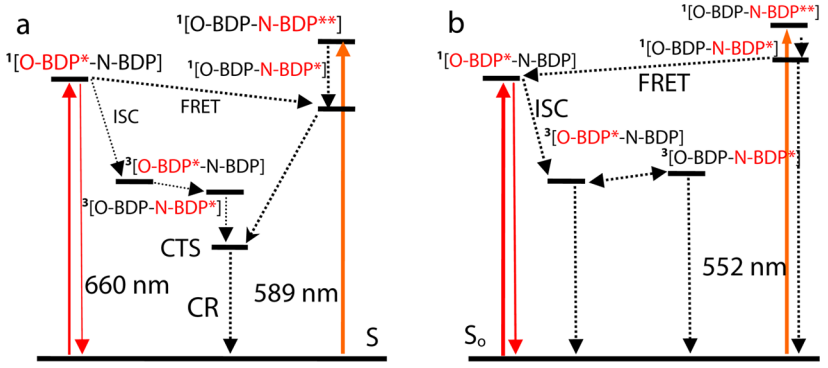

[a][O-BDP-N-Bodipy] stands for **B-2** (O-BDP stands for the Bodipy part with the hydroxyl group, and N-BDP stands for the Bodipy part with the dimethylamino group). The component at the excited state was designated with red color and an asterisk. The number of the superscript designated either the singlet or the triplet excited state. ^{1}[O-BDP-N-BDP**] represents the unrelaxed S_1 state (vertical excitation), ^{1}[O-BDP-N-BDP*] stands for relaxed S_1 state, to indicate the large Stokes shift of **B-2**.

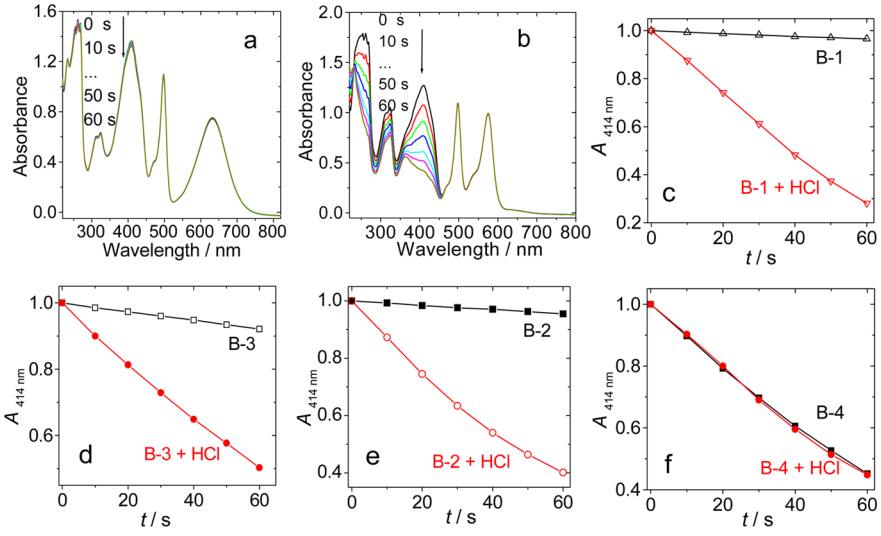

Figure 11. Switching of the singlet oxygen ($^1O_2$) photosensitizing ability of the compounds by aqueous HCl. The decreasing of the absorption of 1,3-diphenylisobenzofuran (DPBF, $^1O_2$ scavenger) was monitored upon monochromic light irradiation. UV−vis absorption spectral changes of the mixture of DPBF and photosensitizer **B-1** upon photoirradiation (a) in the absence of acid and (b) in the presence of acid. The change of the absorption of DPBF at 414 nm with different photosensitizers of (c) **B-1** (λ_{ex} = 592 nm), (d) **B-3** (λ_{ex} = 590 nm), (e) **B-2** (λ_{ex} = 683 nm), (f) **B-4** (λ_{ex} = 663 nm). *c* [DPBF] = 4.5 × 10^{-5} M; *c* [photosensitizers] = 1.0 × 10^{-5} M in CH_3CN/H_2O (9/1, v/v), 20 °C.

room temperature (rt) and water (50 mL) was added. The mixture was extracted with dichloromethane (3 × 50 mL), and the organic layer was dried over anhydrous Na_2SO_4. After removal of the solvent under reduced pressure, the mixture was purified by column chromatography (silica gel, DCM/PE = 2:1, v/v) to give 86.8 mg of deep black solid (yield, 57%). Mp > 250 °C. ^{1}H NMR (400 MHz, $CDCl_3$): δ = 8.18 (d, 1H, *J* = 16.0 Hz), 7.72−7.52 (m, 4H), 7.20 (d, 2H, *J* = 8.8 Hz), 7.13 (d, 2H, *J* = 8.8 Hz), 6.83 (s, 1H), 4.79 (s, 2H), 3.09 (s, 6H), 2.68 (s, 3H), 2.59 (s, 1H), 1.49 (s, 3H), and 1.44 ppm (s, 3H). ^{13}C NMR (125 MHz, $CDCl_3$): δ = 167.7, 158.3, 132.8, 132.3, 130.9, 129.5, 129.4, 129.3, 128.8, 128.1, 115.9, 65.6, 56.0, 31.9, 30.6, 29.7, 29.4, 19.2, 14.1, 13.7 ppm. MALDI-HRMS ($[C_{31}H_{28}BF_2N_3OI_2]^+$): calcd *m*/*z* = 761.0383, found *m*/*z* = 761.0327.

3.3. Synthesis of B-1. A mixture of compound **2** (38.5 mg, 0.05 mmol) and compound **3** (24.1 mg, 0.06 mmol) was dissolved in $CHCl_3$/ethanol/water (12/1/1, v/v, 14 mL) and triethylamine (3 drops). Then $CuSO_4{\cdot}5H_2O$ (0.010 mmol, 3.0 mg) and sodium ascorbate (0.010 mmol, 2 mg) were added. The reaction mixture was stirred at rt for 24 h. After completion of the reaction, water (20 mL) was added and the mixture was extracted with dichloromethane (3 × 30 mL) and the organic layer was dried over anhydrous Na_2SO_4. After removal of the solvent under reduced pressure, the mixture was purified by column chromatography (silica gel, DCM/methanol = 80:1, v/v) to give 50.1 mg of deep black solid (yield, 87%). Mp, 188.8−191.8 °C. ^{1}H NMR: δ = 8.21 (d, 1H, *J* = 16.0 Hz), 7.97 (s, 1H), 7.59−7.50 (m, 3H), 7.21−7.13 (m, 6H), 7.01 (d, 2H, *J* = 8.4 Hz), 6.74 (s, 2H), 5.98 (s, 2H), 5.31 (s, 2H), 4.89−4.87 (m, 2H), 4.48−4.46 (m, 2H), 3.06 (s, 6H), 2.68 (s, 3H), 2.55 (s, 6H), 1.48 (s, 3H), 1.43 (s, 3H), 1.40 ppm (s, 6H). ^{13}C NMR (100 MHz, $CDCl_3$) δ = 159.3, 158.4, 155.6, 146.5, 143.1, 143.0, 141.3, 132.9, 132.1, 132.0, 131.9, 129.7, 129.6, 129.5, 128.4, 128.1, 121.4, 115.7, 115.2, 66.6, 62.1, 50.1, 20.8, 17.9, 17.3, 16.3, 14.8 ppm. MALDI-HRMS ($[C_{52}H_{50}B_2F_4N_8O_2I_2]^+$): cacld *m*/*z* = 1170.2269, found *m*/*z* = 1170.2303.

3.4. Synthesis of B-3. Under Ar atmosphere, a mixture of compound **5** (115.5 mg, 0.2 mmol) and 4-*N*,*N*-dimethylbenzaldehyde (124 mg, 0.8 mmol) was dissolved in dry toluene (20 mL), then 0.2 mL acetic acid (0.2 mL) and piperidine (0.2 mL) were added. The mixture was refluxed for 10 h. After completion of the reaction, the reaction mixture was cooled to rt, water (50 mL) was added. The

dx.doi.org/10.1021/jo5019014 | J. Org. Chem. 2014, 79, 10240−10255

Table 9. Triplet State Lifetimes and Singlet Oxygen Quantum Yields of Photosensitizers B-1−B-4 in the Absence and Presence of Acid

	τ_T (μs)	Φ_Δ[c]
B-1	4.0[a]	7.0[d]/6.9[e]
B-2	1.6[a]	6.0[f]/6.3[g]
B-3	4.4[a]	5.5[e]
B-4	1.7[a]	52.7[g]
	In the Presence of HCl	
B-1	3.1[b]	73.8[d]/69.0[e]
B-2	1.6[b]	59.2[f]/56.3[g]
B-3	6.6[b]	79.8[e]
B-4	1.5[b]	52.7[g]

[a]Triplet lifetime in deaerated toluene. [b]Triplet lifetime in deaerated MeCN/H_2O. [c]Singlet oxygen quantum yield ($^1O_2$). For the peak at shorter wavelength, use diiodoBodipy as the standard (Φ_Δ = 0.82 in CH_2Cl_2); for the peak with longer wavelength use MB as the standard (Φ_Δ = 0.57 in CH_2Cl_2). [d]λ_{ex} = 500 nm. [e]λ_{ex} = 590 nm. [f]λ_{ex} = 562 nm. [g]λ_{ex} = 683 nm.

mixture was extracted with dichloromethane (3 × 50 mL). After removal of the solvent under reduced pressure, the mixture was purified by column chromatography (silica gel, DCM/PE, 2:1, v/v) to give 87.7 mg deep black solid (yield, 62%). Mp > 250 °C. ^{1}H NMR (400 MHz, $CDCl_3$): δ = 8.18 (d, 1H, J = 16.0 Hz), 7.60−7.52 (m, 8H), 6.79 (s, 2H), 3.09 (s, 6H), 2.69 (s, 3H), 1.43 (s, 3H), 1.38 ppm (s, 3H). ^{13}C NMR (100 MHz, $CDCl_3$): δ 154.9, 151.8, 151.3, 146.5, 143.3, 140.5, 138.8, 135.3, 132.5, 131.4, 129.4, 129.3, 128.3, 125.0, 114.0, 112.2, 85.2, 82.7, 40.3, 17.5, 16.8, 16.1. MALDI-HRMS ($[C_{28}H_{26}BF_2N_3I_2]^+$): calcd m/z = 707.0277, found m/z = 707.0327.

3.5. Synthesis of 6. Under Ar atmosphere, a mixture of compound **5** (115.5 mg, 0.2 mmol) and 4-propynylalkoxybenzaldehyde (32 mg, 0.2 mmol) was dissolved in dry toluene (10 mL), then acetic acid (0.1 mL) and piperidine (0.1 mL) were added. The mixture was refluxed for 0.5 h. After completion of the reaction, the reaction mixture was cooled to rt and water (20 mL) was added. The mixture was extracted with dichloromethane (3 × 20 mL) and the organic layer was dried over anhydrous Na_2SO_4. After removal of the solvent under reduced pressure, the mixture was purified by column chromatography (silica gel, DCM/PE = 1:1, v/v) to give 21.5 mg of deep purple solid (yield, 15%). Mp, 178.4−181.2 °C. ^{1}H NMR (400 MHz, $CDCl_3$): δ = 8.14 (d, 1 H, J = 20.0 Hz), 7.62−7.53 (m, 8H), 7.02 (d, 2H, J = 8.0 Hz), 4.75 (d, 2H, J = 4.0 Hz), 2.69 (s, 3H), 2.55 (s, 1H), 1.44 (s, 3H), 1.39 ppm (s, 3H). ^{13}C NMR (125 MHz, $CDCl_3$): 158.5, 157.8, 157.0, 150.4, 138.7, 134.9, 134.8, 130.3, 129.5, 129.4, 129.3, 129.2, 129.1, 128.0, 127.8, 122.3, 117.0, 115.2, 53.8, 38.1, 31.9, 29.7, 17.4, 16.6, 14.6, 14.1 ppm. MALDI-HRMS ($[C_{29}H_{23}BF_2N_2OI_2]^+$): calcd m/z = 717.9961, found m/z = 718.0004.

3.6. Synthesis of B-4. Under Ar atmosphere, a mixture of **6** (22.1 mg, 0.2 mmol) and 4-hydroxybenzaldehyde (4.8 mg, 0.04 mmol) was dissolved in dry toluene (10 mL), then acetic acid (0.05 mL) and piperidine (0.05 mL) were added. The mixture was refluxed for 0.5 h. After completion of the reaction, the reaction mixture was cooled to rt and water (10 mL) was added. The mixture was extracted with dichloromethane (3 × 20 mL) and the organic layer is dried over anhydrous Na_2SO_4. After removal of the solvent under reduced pressure, the mixture was purified by column chromatography (silica gel, DCM/methanol, 70:1 v/v) to give 21.9 mg of deep black solid (yield, 89%). Mp, 248.1−250.1 °C. ^{1}H NMR (400 MHz, $CDCl_3$): δ = 8.15 (d, 2H, J = 20.0 Hz), 7.64−7.53 (m, 9H), 7.30−7.28 (m, 2H), 7.03 (d, 2H, J = 8.0 Hz), 6.90−6.87 (d, 2H, J = 12.0 Hz), 5.07 (s, 1H), 4.75−4.74 (s, 2H), 2.56 (s, 1H), 1.45 ppm (s, 6H). ^{13}C NMR (100 MHz, $CDCl_3$) δ = 175.6, 169.5, 163.1, 158.6, 158.2, 151.1, 150.2, 146.2, 145.5, 139.9, 138.8, 138.5, 135.4, 135.2, 133.0, 132.8, 132.5, 130.5, 129.7, 129.6, 129.3, 129.0, 128.5, 117.3, 116.1, 115.3, 55.8, 47.7, 42.9, 26.5, 24.5 ppm. MALDI -HRMS ($[C_{36}H_{27}BF_2N_2O_2I_2]^+$): calcd m/z = 822.0223, found m/z = 822.0270.

3.7. Synthesis of 4. Under Ar atmosphere, a mixture of compound **3** (80.2 mg, 0.2 mmol) and 4-*N*,*N*-dimethylbenzaldehyde (124 mg, 0.8 mmol) was dissolved in dry toluene (20 mL), then 0.2 mL of acetic acid and 0.2 mL of piperidine were added. The mixture was refluxed for 12 h. After completion of the reaction, the mixture was cooled to rt. Water (10 mL) was added, and the mixture was extracted with dichloromethane (3 × 50 mL). After removal of the solvent under reduced pressure, the mixture was purified by column chromatography (silica gel, DCM/methanol = 70:1, v/v) to give 47.4 mg of deep black solid (yield, 49%). Mp, 256.6−257.6 °C. ^{1}H NMR (400 MHz, $CDCl_3$): δ = 7.57 (d, 3H, J = 8.0 Hz), 7.23−7.18 (m, 3H), 7.05 (d, 2H, J = 7.8 Hz), 6.84 (s, 2H), 6.60 (s, 1H), 5.99 (s, 1H), 4.23−4.20 (m, 2H), 3.68−3.66 (m, 2H), 3.07 (s, 6H), 2.59 (s, 3H), 1.48 (s, 3H), 1.44 ppm (s, 3H). MALDI-HRMS ($[C_{30}H_{31}BF_2N_6O]^+$): calcd m/z = 540.2620, found m/z = 540.2637.

3.8. Synthesis of B-2. Under Ar atmosphere, a mixture of compound **4** (12.5 mg, 0.03 mmol) and compound **B-4** (16.4 mg, 0.02 mmol) was dissolved in $CHCl_3$/ethanol/water (12/1/1, v/v, 14 mL) and 3 drops of triethylamine was added. Then $CuSO_4{\cdot}5H_2O$ (0.010 mmol, 3.0 mg) and sodium ascorbate (0.010 mmol, 2 mg) were added. The reaction mixture was stirred for 24 h at rt. After completion of the reaction, water (20 mL) was added. The mixture was extracted with dichloromethane (3 × 30 mL), and the organic layer is dried over Na_2SO_4. After removal of the solvent under reduced pressure, the mixture was purified by column chromatography (silica gel, DCM/methanol = 60:1, v/v) to give 22.1 mg of deep black solid (yield, 81%). Mp > 250 °C. ^{1}H NMR (400 MHz, $CDCl_3$): δ = 8.12 (d, 2H, J = 16.0 Hz), 7.85 (s, 1H), 7.60−7.48 (m, 11H), 7.19−7.15 (m, 3H), 7.03 (d, 3H, J = 8.0 Hz), 6.90−6.88 (m, 4H), 6.72 (s, 2H), 6.56 (s, 1H), 5.94 (s, 1H), 5.80 (s, 1H), 5.30 (s, 2H), 4.82−4.80 (m, 2H), 4.41−4.39 (m, 2H), 3.04 (s, 6H), 2.55 (s, 3H), 1.56 (s, 3H), 1.40−1.38 ppm (m, 9H). ^{13}C NMR (100 MHz, $CDCl_3$) δ = 169.0, 162.2, 158.9, 158.1, 157.5, 154.7, 152.7, 151.0, 150.6, 147.4, 145.9, 145.7, 144.2, 142.8, 141.4, 140.6, 139.3, 138.5, 138.3, 137.8, 135.3, 133.4, 132.3, 132.0, 131.4, 130.2, 129.9, 129.6, 129.4, 129.3, 128.4, 124.2, 120.4, 117.8, 117.2, 116.4, 116.0, 115.9, 114.9, 114.2, 112.0, 66.3, 61.9, 47.5, 42.6, 40.2, 29.7, 26.4, 25.5, 24.4, 21.5 ppm. MALDI-HRMS ($[C_{66}H_{58}B_2F_4N_8O_3I_2]^+$): calcd m/z = 1362.2844, found m/z = 1362.2787.

3.9. Nanosecond Time-Resolved Transient Difference Absorption Spectra. The spectra were measured on LP920 laser flash photolysis spectrometer (Edinburgh Instruments, U.K.), and the signal was buffered on a Tektronix TDS 3012B oscilloscope. The lifetime values (by monitoring the decay trace of the transients) were calculated with the LP900 software. All samples in the flash photolysis experiments were deaerated with N_2 for ∼15 min before measurement, and the gas flow is kept during the measurement.

■ ASSOCIATED CONTENT

Supporting Information

Experimental procedures, molecular structure characterization, and additional spectra. This material is available free of charge via the Internet at http://pubs.acs.org.

■ AUTHOR INFORMATION

Corresponding Author

*E-mail: zhaojzh@dlut.edu.cn.

Notes

The authors declare no competing financial interest.

■ ACKNOWLEDGMENTS

We thank the NSFC (Grants 21273028, 21473020, and 21421005), the Royal Society (U.K.) and NSFC (Cost-Share-21011130154), Ministry of Education (Grant SRFDP-20120041130005), the Fundamental Research Funds for the Central Universities (Grant DUT14ZD226), Dalian University of Technology (DUT2013TB07), and Program for Changjiang

Scholars and Innovative Research Team in University [Grant IRT_132206] for financial support.

REFERENCES

(1) Prier, C. K.; Rankic, D. A.; MacMillan, D. W. C. *Chem. Rev.* **2013**, *113*, 5322−5363.
(2) Narayanam, J. M. R.; Stephenson, C. R. J. *Chem. Soc. Rev.* **2011**, *40*, 102−113.
(3) Shi, L.; Xia, W. *Chem. Soc. Rev.* **2012**, *41*, 7687−7697.
(4) Xi, Y.; Yi, H.; Lei, A. *Org. Biomol. Chem.* **2013**, *11*, 2387−2403.
(5) Ravelli, D.; Fagnoni, M.; Albini, A. *Chem. Soc. Rev.* **2013**, *42*, 97−113.
(6) Zhao, J.; Wu, W.; Sun, J.; Guo, S. *Chem. Soc. Rev.* **2013**, *42*, 5323−5351.
(7) McDonnell, S. O.; Hall, M. J.; Allen, L. T.; Byrne, A.; Gallagher, W. M.; O'Shea, D. F. *J. Am. Chem. Soc.* **2005**, *127*, 16360−16361.
(8) Yogo, T.; Urano, Y.; Ishitsuka, Y.; Maniwa, F.; Nagano, T. *J. Am. Chem. Soc.* **2005**, *127*, 12162−12163.
(9) Ozlem, S.; Akkaya, E. U. *J. Am. Chem. Soc.* **2009**, *131*, 48−49.
(10) Schmitt, F.; Freudenreich, J.; Barry, N. P. E.; Juillerat-Jeanneret, L.; Süss-Fink, G.; Therrien, B. *J. Am. Chem. Soc.* **2012**, *134*, 754−757.
(11) Kamkaew, A.; Lim, S. H.; Lee, H. B.; Kiew, L. V.; Chung, L. Y.; Burgess, K. *Chem. Soc. Rev.* **2013**, *42*, 77−88.
(12) Awuah, S. G.; You, Y. *RSC Adv.* **2012**, *2*, 11169−11183.
(13) (a) Adarsh, N.; Avirah, R. R.; Ramaiah, D. *Org. Lett.* **2010**, *12*, 5720−5723. (b) Niedermair, F.; Borisov, S. M.; Zenkl, G.; Hofmann, O. T.; Weber, H.; Saf, R.; Klimant, I. *Inorg. Chem.* **2010**, *49*, 9333−9342.
(14) Guo, H.; Ji, S.; Wu, W.; Wu, W.; Shao, J.; Zhao, J. *Analyst* **2010**, *135*, 2832−2840.
(15) Lazarides, T.; McCormick, T. M.; Wilson, K. C.; Lee, S.; McCamant, D. W.; Eisenberg, R. *J. Am. Chem. Soc.* **2011**, *133*, 350−364.
(16) Yukruk, F.; Dogan, A. L.; Canpinar, H.; Guc, D.; Akkay, E. U. *Org. Lett.* **2005**, *7*, 2885−2887.
(17) Duman, S.; Cakmak, Y.; Kolemen, S.; Akkaya, E. U.; Dede, Y. *J. Org. Chem.* **2012**, *77*, 4516−4527.
(18) Sabatini, R. P.; McCormick, T. M.; Lazarides, T.; Wilson, K. C.; Eisenberg, R.; McCamant, D. W. *J. Phys. Chem. Lett.* **2011**, *2*, 223−227.
(19) de Silva, A. P.; Gunaratne, H. Q. N.; Gunnlaugsson, T.; Huxley, A. J. M.; McCoy, C. P.; Rademacher, J. T.; Rice, T. E. *Chem. Rev.* **1997**, *97*, 1515−1566.
(20) (a) Chen, Y.; Qi, D.; Zhao, L.; Cao, W.; Huang, C.; Jiang, J. *Chem.—Eur. J.* **2013**, *19*, 7342−7347. (b) Wang, G. K.; Mi, Q. L.; Zhao, L. Y.; Hu, J. J.; Guo, L. E.; Zou, X. J.; Liu, B.; Xie, X. G.; Zhang, J. F.; Zhao, Q. H.; Zhou, Y. *Chem.−Asian J.* **2014**, *9*, 744−748. (c) Rajeswara R, M.; Liao, C.-W.; Sun, S.-S. *J. Mater. Chem. C* **2013**, *1*, 6386−6394.
(21) Fan, J.; Hu, M.; Zhan, P.; Peng, X. *Chem. Soc. Rev.* **2013**, *42*, 29−43.
(22) Ziessel, R.; Harriman, A. *Chem. Commun.* **2011**, *47*, 611−631.
(23) Guliyev, R.; Coskun, A.; Akkaya, E. U. *J. Am. Chem. Soc.* **2009**, *131*, 9007−9013.
(24) Bura, T.; Nastasi, F.; Puntoriero, F.; Campagna, S.; Ziessel, R. *Chem.—Eur. J.* **2013**, *19*, 8900−8912.
(25) Yuan, L.; Lin, W.; Zheng, K.; Zhu, S. *Acc. Chem. Res.* **2013**, *46*, 1462−1473.
(26) Lee, M. H.; Han, J. H.; Lee, J. H.; Park, N.; Kumar, R.; Kang, C.; Kim, J. S. *Angew. Chem., Int. Ed.* **2013**, *125*, 6326−6329.
(27) El-Khouly, M. E.; Amin, A. N.; Zandler, M. E.; Fukuzumi, S.; D'Souza, F. *Chem.—Eur. J.* **2012**, *18*, 5239−5247.
(28) Loudet, A.; Burgess, K. *Chem. Rev.* **2007**, *107*, 4891−4932.
(29) Bandichhor, R.; Petrescu, A. D.; Vespa, A.; Kier, A. B.; Schroeder, F.; Burgess, K. *J. Am. Chem. Soc.* **2006**, *128*, 10688−10689.
(30) Wan, C.-W.; Burghart, A.; Chen, J.; Bergström, F.; Johansson, L. B.-Å.; Wolford, M. F.; Kim, T. G.; Topp, M. R.; Hochstrasser, R. M.; Burgess, K. *Chem.—Eur. J.* **2003**, *9*, 4430−4441.
(31) Zhao, Y.; Zhang, Y.; Lv, X.; Liu, Y.; Chen, M.; Wang, P.; Liu, J.; Guo, W. *J. Mater. Chem.* **2011**, *21*, 13168−13171.
(32) Qu, X.; Liu, Q.; Ji, X.; Chen, H.; Zhou, Z.; Shen, Z. *Chem. Commun.* **2012**, *48*, 4600−4602.
(33) (a) Erbas-Cakmak, S.; Bozdemir, O. A.; Cakmak, Y.; Akkaya, E. U. *Chem. Sci.* **2013**, *4*, 858−862. (b) Erbas-Cakmak, S.; Akkaya, E. U. *Angew. Chem., Int. Ed.* **2013**, *52*, 11364−11368.
(34) Léaustic, A.; Anxolabéhère-Mallart, E.; Maurel, F.; Midelton, S.; Guillot, R.; Métivier, R.; Nakatani, K.; Yu, P. *Chem.—Eur. J.* **2011**, *17*, 2246−2255.
(35) Tian, J.; Ding, L.; Xu, H.-J.; Shen, Z.; Ju, H.; Jia, L.; Bao, L.; Yu, J.-S. *J. Am. Chem. Soc.* **2013**, *135*, 18850−18858.
(36) He, B.; Wenger, O. S. *Inorg. Chem.* **2012**, *51*, 4335−4342.
(37) Jukes, R. T. F.; Adamo, V.; Hartl, F.; Belser, P.; De Cola, L. *Inorg. Chem.* **2004**, *43*, 2779−2792.
(38) (a) Li, B.; Wang, J.-Y.; Wen, H.-M.; Shi, L.-X.; Chen, Z.-N. *J. Am. Chem. Soc.* **2012**, *134*, 16059−16067. (b) Tan, W.; Zhang, Q.; Zhang, J.; Tian, H. *Org. Lett.* **2009**, *11*, 161−164.
(39) Lin, J.-L.; Chen, C.-W.; Sun, S.-S.; Lees, A. J. *Chem. Commun.* **2011**, *47*, 6030−6032.
(40) Zhang, C.; Zhao, J.; Wu, S.; Wang, Z.; Wu, W.; Ma, J.; Guo, S.; Huang, L. *J. Am. Chem. Soc.* **2013**, *135*, 10566−10578.
(41) Guo, S.; Ma, J.; Zhao, J.; Küçüköz, B.; Karatay, A.; Hayvali, M.; Yaglioglub, H. G.; Elmali, A. *Chem. Sci.* **2014**, *5*, 489−500.
(42) Huang, L.; Cui, X.; Therrien, B.; Zhao, J. *Chem.—Eur. J.* **2013**, *19*, 17472−17482.
(43) Huang, L.; Yu, X.; Wu, W.; Zhao, J. *Org. Lett.* **2012**, *14*, 2594−2597.
(44) Ulrich, G.; Ziessel, R.; Harriman, A. *Angew. Chem., Int. Ed.* **2008**, *47*, 1184−1201.
(45) Benniston, A. C.; Copley, G. *Phys. Chem. Chem. Phys.* **2009**, *11*, 4124−4131.
(46) Ni, Y.; Zeng, W.; Huang, K.-W.; Wu, J. *Chem. Commun.* **2013**, *49*, 1217−1219.
(47) Bura, T.; Retailleau, P.; Ulrich, G.; Ziessel, R. *J. Org. Chem.* **2011**, *76*, 1109−1117.
(48) Poirel, A.; De Nicola, A.; Retailleau, P.; Ziessel, R. *J. Org. Chem.* **2012**, *77*, 7512−7525.
(49) Li, W.; Lin, W.; Wang, J.; Guan, X. *Org. Lett.* **2013**, *15*, 1768−1771.
(50) Wu, W.; Zhao, J.; Sun, J.; Guo, S. *J. Org. Chem.* **2012**, *77*, 5305−5312.
(51) Yang, P.; Wu, W.; Zhao, J.; Huang, D.; Yi, X. *J. Mater. Chem.* **2012**, *22*, 20273−20283.
(52) Huang, D.; Zhao, J.; Wu, W.; Yi, X.; Yang, P.; Ma, J. *Asian J. Org. Chem.* **2012**, *1*, 264−273.
(53) Chen, Y.; Zhao, J.; Guo, H.; Xie, L. *J. Org. Chem.* **2012**, *77*, 2192−2206.
(54) Liu, Y.; Zhao, J. *Chem. Commun.* **2012**, *48*, 3751−3753.
(55) Bozdemir, O. A.; Erbas-Cakmak, S.; Ekiz, O. O.; Dana, A.; Akkaya, E. U. *Angew. Chem., Int. Ed.* **2011**, *50*, 10907−10912.
(56) Yin, S.; Leen, V.; Jackers, C.; Beljonne, D.; Averbeke, B. V.; der Auweraer, M. V.; Boens, N.; Dehaen, W. *Chem.—Eur. J.* **2011**, *17*, 13247−13257.
(57) Zhang, D.; Martín, V.; García-Moreno, I.; Costel, A.; Pérez-Ojeda, M. E.; Xiao, Y. *Phys. Chem. Chem. Phys.* **2011**, *13*, 13026−13033.
(58) Yuan, M.; Yin, X.; Zheng, H.; Ouyang, C.; Zuo, Z.; Liu, H.; Li, Y. *Chem.—Asian J.* **2009**, *4*, 707−713.
(59) (a) Baruah, M.; Qin, W.; Flors, C.; Hofkens, J.; Vallée, R. A. L.; Beljonne, D.; der Auweraer, M. V.; De Borggraeve, W. M.; Boens, N. *J. Phys. Chem. A* **2006**, *110*, 5998−6009. (b) Hong, Y.; Liao, J.-Y.; Cao, D.; Zang, X.; Kuang, D.-B.; Wang, L.; Meier, H.; Su, C.-Y. *J. Org. Chem.* **2011**, *76*, 8015−8021.
(60) (a) Wu, W.; Guo, H.; Wu, W.; Ji, S.; Zhao, J. *J. Org. Chem.* **2011**, *76*, 7056−7064. (b) Rachford, A. A.; Ziessel, R.; Bura, T.; Retailleau, P.; Castellano, F. N. *Inorg. Chem.* **2010**, *49*, 3730−3736.
(61) Kostereli, Z.; Ozdemir, T.; Buyukcakir, O.; Akkaya, E. U. *Org. Lett.* **2012**, *14*, 3636−3639.

(62) Shao, J.; Guo, H.; Ji, S.; Zhao, J. *Biosens. Bioelectron.* **2011**, *26*, 3012−3017.
(63) Guo, H.; Jing, Y.; Yuan, X.; Ji, S.; Zhao, J.; Li, X.; Kan, Y. *Org. Biomol. Chem.* **2011**, *9*, 3844−3853.
(64) Quartarolo, A. D.; Russo, N.; Sicilia, E. *Chem.—Eur. J.* **2006**, *12*, 6797−6803.
(65) Kand, D.; Mishra, P. K.; Saha, T.; Lahiri, M.; Talukdar, P. *Analyst* **2012**, *137*, 3921−3924.
(66) Ziessel, R.; Allen, B. D.; Rewinska, D. B.; Harriman, A. *Chem.—Eur. J.* **2009**, *15*, 7382−7393.
(67) Puntoriero, F.; Nastasi, F.; Campagna, S.; Bura, T.; Ziessel, R. *Chem.—Eur. J.* **2010**, *16*, 8832−8845.
(68) Takizawa, S.; Aboshi, R.; Murata, S. *Photochem. Photobiol. Sci.* **2011**, *10*, 895−903.
(69) Bura, T.; Retailleau, P.; Ulrich, G.; Ziessel, R. *J. Org. Chem.* **2011**, *76*, 1109−1117.